The EMBO Journal (2012) 31, 788–804 | © 2012 European Molecular Biology Organization | All Rights Reserved 0261-4189/12
www.embojournal.org

THE EMBO JOURNAL

Mechanoinduction of lymph vessel expansion

Lara Planas-Paz[1,2], Boris Strilić[1,6], Axel Goedecke[3], Georg Breier[4], Reinhard Fässler[5] and Eckhard Lammert[1,*]

[1]Institute of Metabolic Physiology, Heinrich-Heine University, Düsseldorf, Germany, [2]Max Planck Institute of Molecular Cell Biology and Genetics, Dresden, Germany, [3]Institute of Cardiovascular Physiology, Heinrich-Heine University, Düsseldorf, Germany, [4]Institute of Pathology, Medical Faculty, DFG Research Center and Cluster of Excellence for Regenerative Therapies, University of Technology, Dresden, Germany and [5]Department of Molecular Medicine, Max Planck Institute of Biochemistry, Martinsried, Germany

In the mammalian embryo, few mechanical signals have been identified to influence organ development and function. Here, we report that an increase in the volume of interstitial or extracellular fluid mechanically induces growth of an organ system, that is, the lymphatic vasculature. We first demonstrate that lymph vessel expansion in the developing mouse embryo correlates with a peak in interstitial fluid pressure and lymphatic endothelial cell (LEC) elongation. In '*loss-of-fluid*' experiments, we then show that aspiration of interstitial fluid reduces the length of LECs, decreases tyrosine phosphorylation of vascular endothelial growth factor receptor-3 (VEGFR3), and inhibits LEC proliferation. Conversely, in '*gain-of-fluid*' experiments, increasing the amount of interstitial fluid elongates the LECs, and increases both VEGFR3 phosphorylation and LEC proliferation. Finally, we provide genetic evidence that β1 integrins are required for the proliferative response of LECs to both fluid accumulation and cell stretching and, therefore, are necessary for lymphatic vessel expansion and fluid drainage. Thus, we propose a new and physiologically relevant mode of VEGFR3 activation, which is based on mechanotransduction and is essential for normal development and fluid homeostasis in a mammalian embryo.

The EMBO Journal (2012) **31,** 788–804. doi:10.1038/emboj.2011.456; Published online 13 December 2011
Subject Categories: cell & tissue architecture; development
Keywords: β1 integrin; fluid homeostasis; lymphatic vessel; mouse embryo; VEGFR3 signalling

Introduction

Two interconnected organ systems, the blood vasculature and lymphatic vasculature, are of particular interest from both a biological and a medical point of view, since they are abundant and exert vital functions in vertebrate tissues during development, health, and disease (reviewed by Affolter *et al*, 2009; Tammela and Alitalo, 2010; Wang and Oliver, 2010 and Schulte-Merker *et al*, 2011). Whereas the blood vasculature delivers blood cells and plasma fluid to virtually all tissues, the lymphatic vasculature removes interstitial fluid, which accumulates within the tissues due to transvascular fluid passage (reviewed by Földi and Strössenreuther, 2005 and Rutkowski and Swartz, 2007). With few exceptions, plasma flows via the arterial blood stream to any given tissue. Part of the plasma fluid leaks out of the blood vessels, and the fluid that does not re-enter the capillaries flows through the interstitium to the lymph vessels (reviewed by Rutkowski and Swartz, 2007). The latter absorb the interstitial fluid and transport it back to the blood vasculature, thus closing the fluid cycle in the living organism. In healthy adult humans, lymph vessels remove up to 2 L of fluid each day from all tissues (reviewed by Földi and Strössenreuther, 2005).

Lymph vessels are formed by lymphatic endothelial cells (LECs), which differ from blood vascular endothelial cells (VECs) by the expression of a number of molecular markers, including Lyve-1, Prox1 and vascular endothelial growth factor receptor-3 (VEGFR3) (reviewed by Wang and Oliver, 2010 and Schulte-Merker *et al*, 2011). In addition, lymph vessels are attached to the surrounding extracellular matrix (ECM) via anchoring filaments and integrins that play a role in the drainage of interstitial fluid from the surrounding tissues (reviewed by Mäkinen *et al*, 2007 and Garmy-Susini and Varner, 2008). When the interstitial fluid pressure rises, LECs are stretched due to changes in the surrounding ECM that they adhere to, and their intercellular junctions are opened to absorb interstitial fluid (reviewed by Mäkinen *et al*, 2007; Tammela and Alitalo, 2010; Schulte-Merker *et al*, 2011). Thus, according to the current model, stretching of LECs in response to an increased interstitial fluid pressure is key to the removal of extracellular fluid from vertebrate tissues.

To date, lymphatic development has been best studied in the developing mouse embryo. Similarly to other vertebrates studied so far, in mice LECs start to differentiate from VECs of the cardinal veins (Ny *et al*, 2005; Küchler *et al*, 2006; Yaniv *et al*, 2006; Srinivasan *et al*, 2007; Hogan *et al*, 2009). Subsequently, the LECs migrate dorsolaterally into the surrounding mesenchyme in order to form irregularly shaped primary lymph sacs. The first lymph sacs to form in the mouse embryo are the 'jugular lymph sacs' (jls), which develop adjacent to the anterior cardinal veins (acv) at around E11.0–E11.5 of mouse development (Figure 1; reviewed by Mäkinen *et al*, 2007; Schulte-Merker *et al*, 2011). Once the jls have formed, they expand in size from E11.5 onwards, start to sprout at E13.5, and finally develop into a mature lymphatic vasculature at later embryonic stages (reviewed by Mäkinen *et al*, 2007; Tammela and Alitalo, 2010; Schulte-Merker *et al*, 2011).

More than 20 genes have been identified to be involved in various steps of embryonic lymphatic development, including

*Corresponding author: Institute of Metabolic Physiology, Heinrich-Heine University, Düsseldorf 40225, Germany. Tel.: +49 2118114990; Fax: +49 2118113897; E-mail: lammert@uni-duesseldorf.de
[6]Present address: Department of Pharmacology, Max Planck Institute for Heart and Lung Research, W.G. Kerckhoff-Institute, 61231 Bad Nauheim, Germany

Received: 11 July 2011; accepted: 14 November 2011; published online: 13 December 2011

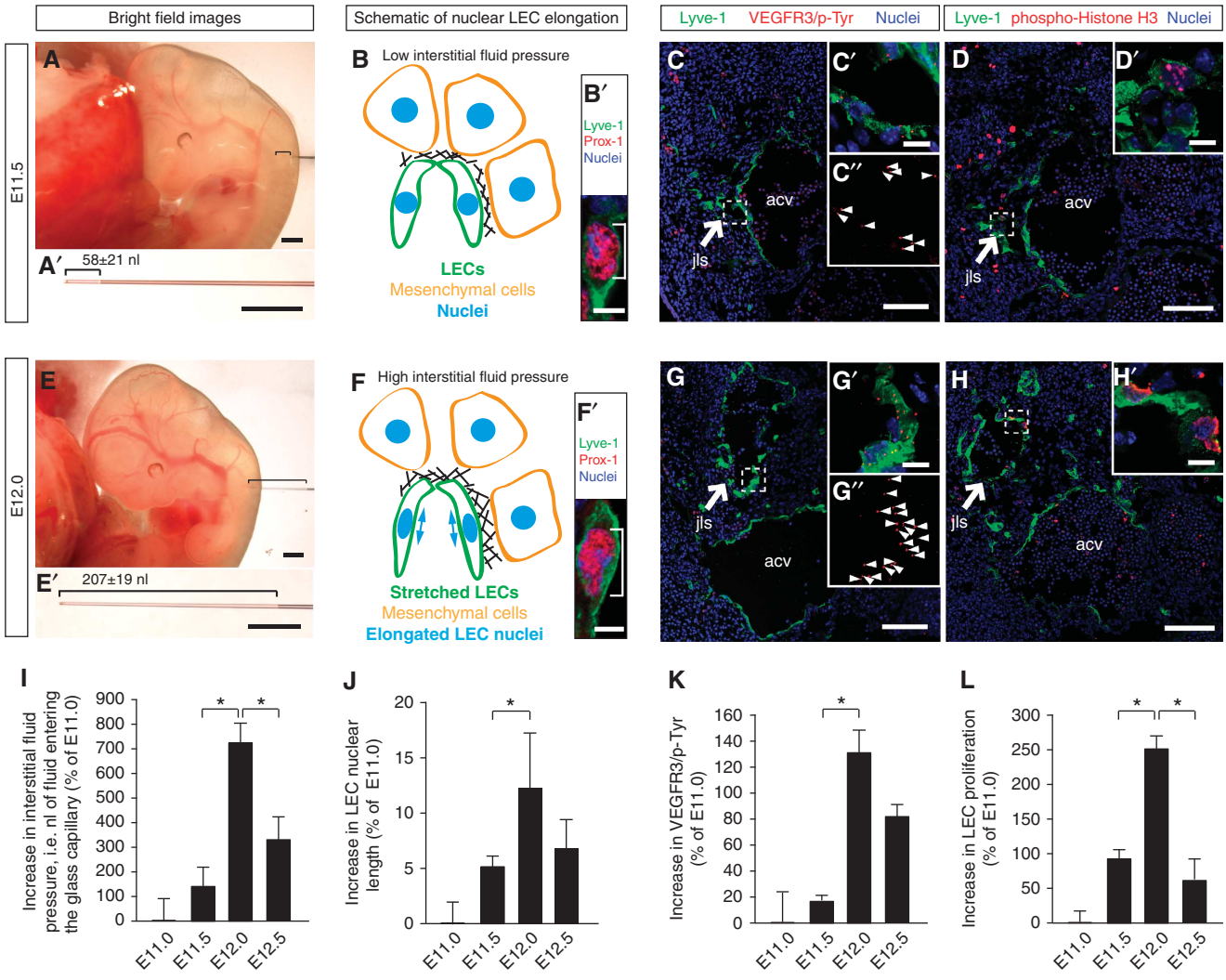

Figure 1 Interstitial fluid pressure and lymphatic endothelial cell elongation correlate with lymph vessel expansion in the developing mouse embryo. (**A**, **E**) Representative bright field images of (**A**) E11.5 and (**E**) E12.0 wild-type mouse embryos. A glass micro-capillary was inserted into the mesenchyme in which a jugular lymph sac (jls) develops, and the nanoliters of interstitial fluid that entered the glass capillary were measured. The amount of interstitial fluid entering the glass capillary at E11.5 and E12.0 is displayed in (**A′**) and (**E′**), respectively. Scale bars, 500 μm. (**B**, **F**) Schematic illustration of LEC stretching and nuclear elongation at (**B**) E11.5 and (**F**) E12.0 of mouse embryonic development. (**B′**, **F′**) Laser scanning microscopy (LSM) images of LECs immunostained for the lymphatic markers Lyve-1 (green) and Prox-1 (red) to visualize the nuclear elongation at (**B′**) E11.5 and (**F′**) E12.0 of mouse embryonic development. Scale bars, 5 μm. (**C**, **G**) Representative LSM images of proximity ligation assays (PLA) on cross-sections through the jugular lymph sacs (jls) of wild-type (**C**) E11.5 and (**G**) E12.0 mouse embryos. Arrows point to the jugular lymph sac (jls) immunostained for Lyve-1 (green). The anterior cardinal vein (acv) is also indicated. Scale bars, 100 μm. (**C′**, **C″**, **G′**, **G″**) Magnification of (**C**) and (**G**). Red staining (arrowheads) indicates sites of VEGFR3 with phosphorylated tyrosines. Scale bars, 10 μm. (**D**, **H**) Cross-sections through the jugular lymph sac (jls) of representative wild-type (**D**) E11.5 and (**H**) E12.0 mouse embryos, immunostained for Lyve-1 (green), proliferation marker phospho-histone H3 (red) and nuclei (DAPI, blue). Scale bars, 100 μm. (**D′**, **H′**) Magnification of (**D**) and (**H**). Scale bars, 10 μm. (**I**) Increase in interstitial fluid pressure in wild-type mouse embryos at the indicated stages of embryonic development. Interstitial fluid pressure was measured as the nanoliters of fluid entering a glass capillary. All values are means ± s.d., $n \geqslant 11$ embryos per stage, $^*P < 0.05$ (first bracket: $P = 0.001$, second bracket: $P = 0.038$). (**J**) Increase in LEC nuclear length in wild-type mouse embryos at the indicated stages of embryonic development. All values are means ± s.d., $n = 130$–300 cells per embryo in a total of three embryos per stage, $^*P = 0.032$. (**K**) Increase in sites of VEGFR3 with phosphorylated tyrosines in LECs of wild-type mouse embryos at the indicated stages of embryonic development. All values are means ± s.d., $n = 3$ embryos per stage, $^*P = 0.037$. (**L**) Increase in LEC proliferation in wild-type mouse embryos at the indicated stages of development. All values are means ± s.d., $n \geqslant 3$ embryos per stage, $^*P < 0.05$ (first bracket: $P = 0.004$, second bracket: $P = 0.006$).

the genes for Prox1, Sox18, Coup-TFII, VEGFR3, VEGF-C, Nrp2, Ccbe1, Rac1, Clp24, Tbx1, Ptpn14, Liprin-beta1, Adm, Ramp2, Calcrl, Vezf, Tie1, Meis1, Slp76, Plcg2, Pdpn, C1galt1, Clec-2, Syk, Spred1/Spred2, Akt1, Angpt2, Pi3kca, Pik3r1, Itga9, Fn1, Emilin1, Aspp1, Efnb2, Foxc2, NFATc1, Elk3, and PU.1 (reviewed by Schulte-Merker *et al*, 2011). The majority of these genes code for proteins involved in growth factor- or ligand-induced signalling events. In stark contrast, no mechanical signal has yet been reported to regulate lymphatic development in embryos. In the adult mouse, however, interstitial flow was shown to increase the expression and distribution of VEGF-C and matrix metalloproteinases (MMPs), and to trigger LEC migration during tissue regeneration (reviewed by Rutkowski and Swartz, 2007 and Goldman *et al*, 2007), showing that mechanical signals can influence lymphatic development in the adult.

In general, only a limited number of reports exist on mechanically induced developmental processes in the mammalian embryo (reviewed by le Noble *et al*, 2008; Mammoto and Ingber, 2010; and Schwartz, 2010), which might reflect a shortage of experimental tools needed to study the role of these signals *in vivo*. Here, we designed experiments to identify a correlation between the amount of interstitial fluid, the stretching of LECs, and the extent of lymph vessel expansion in the developing mouse embryo. By using both 'loss-of-fluid' and 'gain-of-fluid' experiments, we show that the fluid volume within the embryonic interstitium controls LEC elongation, VEGFR3 signalling, and LEC proliferation in a β1 integrin-dependent manner. Therefore, we propose a new signalling mechanism, which is based on mechanotransduction and is essential for lymphatic growth and fluid homeostasis in the mammalian embryo.

Results

Correlation between fluid pressure and LEC elongation in the developing mouse embryo

The lymphatic vasculature removes fluid from extracellular spaces. Here, the hypothesis that an increase in interstitial fluid volume induced growth of the developing lymphatic vasculature was investigated. We isolated mouse embryos at different developmental stages and measured the interstitial fluid pressure within the jugular region (Figure 1A and E). The jugular region of the embryos was chosen, because it represents an area where formation and growth of the first primary lymph sacs, called jls take place (reviewed by Srinivasan *et al*, 2007 and Schulte-Merker *et al*, 2011). A glass capillary was inserted into the jugular region of the embryos at different stages of development, and the volumes of fluid that entered the capillary were used as a measure of interstitial fluid pressure (Supplementary Movie S1; Figure 1A, A′, E, and E′). To rule out the puncture of a blood vessel, the fluid volume was only included in the measurements when blood cells were absent within the fluid entering the capillary.

The fluid pressure in the jugular interstitium significantly increased from E11.5 to E12.0 (compare Figure 1A and A′ with Figure 1E and E′; see Figure 1I and Supplementary Movie S1). In contrast, from E12.0 to E12.5 the fluid pressure significantly decreased (Figure 1I). Since a high interstitial fluid pressure results in swelling of the interstitium, leading to a stretching of the ECM and of the adhering LECs (reviewed by Tammela and Alitalo, 2010 and Schulte-Merker *et al*, 2011), we determined the lengths of the LEC nuclei as a measure of cell stretching (compare Figure 1B and B′ with Figure 1F and F′). Cell nuclei are embedded within the cytoskeleton and thus elongate upon cell stretching (reviewed by Friedl *et al*, 2011). As well as the interstitial fluid pressure, the nuclear length of the LECs also increased significantly from E11.5 to E12.0 (Figure 1J) and decreased from E12.0 to E12.5 ($P=0.12$). Together, these data suggest that an increase in interstitial fluid volume leads to a stretching of LECs in the developing mouse embryo.

Correlation between fluid pressure, VEGFR3 signalling, and LEC proliferation

VEGF-C is required for lymph vessel formation (Karkkainen *et al*, 2004). It induces formation of VEGFR3 homodimers and VEGFR3/2 heterodimers in LECs, which in turn result in tyrosine phosphorylation of their intracellular domains (Nilsson *et al*, 2010; Wang *et al*, 2010). The phospho-tyrosines initiate signal transduction cascades, which trigger cellular responses, including cell proliferation (reviewed by Bahram and Claesson-Welsh, 2010). Proximity ligation assays (PLAs; Söderberg *et al*, 2006; Jarvius *et al*, 2007) were used to determine the levels of VEGFR3 tyrosine phosphorylation in LECs, which were stained for Lymphatic vessel hyaluronan receptor-1 (Lyve-1) (Figure 1C and G). PLA signals for VEGFR3 phospho-tyrosines were detected on the LECs (Figure 1C′ and G′). Importantly, the PLA staining significantly increased from E11.5 to E12.0 (compare Figure 1C′ and C″ with Figure 1G′ and G″; see Figure 1K), whereas the staining decreased from E12.0 to E12.5 ($P=0.06$) (Figure 1K). To confirm that the PLA is a reliable readout of VEGFR3 tyrosine phosphorylation, we injected a specific activator of VEGFR3, VEGF-C (C156S), into the jugular region of wild-type embryos (Supplementary Figure S1). As expected, the PLA signals in LECs increased in number

Figure 2 'Loss-of-fluid' experiments: Lowering the interstitial fluid volume reduces LEC elongation, and decreases VEGFR3 tyrosine phosphorylation and LEC proliferation. (**A**, **B**) Representative bright field images of wild-type E11.5 mouse embryos, in which (**A**) 10 nl and (**B**) 100 nl interstitial fluid was removed from the area of lymphatic development. Scale bars, 1 mm. The amount of fluid taken from the interstitium is displayed in (**A**′) and (**B**′). Scale bars, 10 μm. (**C**) Schematic illustration of the removal of interstitial fluid from embryonic tissue using a glass micro-capillary. When the interstitial fluid pressure is reduced, the LECs are less stretched, and their nuclei are less elongated. (**C**′, **C**″) Laser scanning microscopy (LSM) images of LECs immunostained for Lyve-1 (green) and Prox-1 (red) to visualize the nuclear shortening when (**C**″) 100 nl interstitial fluid was removed compared with (**C**′) the removal of 10 nl interstitial fluid. Scale bars, 5 μm. (**D**, **E**, **G**, **H**) Representative LSM images of proximity ligation assays (PLA) on cross-sections through the jugular lymph sacs (jls) of wild-type E11.5 mouse embryos, from which (**D**, **E**) 10 nl or (**G**, **H**) 100 nl interstitial fluid was removed, and cultivated for 30 min in whole embryo culture (WEC). Red staining (arrowheads) indicates sites of VEGFR3 with phosphorylated tyrosines. Co-staining is shown for the lymphatic marker Lyve-1 (green) and nuclei (DAPI, blue). Scale bars, 10 μm. (**F**, **I**) Cross-sections through the jugular lymph sac (jls) of representative wild-type E11.5 mouse embryos, from which (**F**) 10 nl or (**I**) 100 nl interstitial fluid was removed, and immunostained for Lyve-1 (green), proliferation marker phospho-histone H3 (red) and nuclei (DAPI, blue). Proliferating cells are indicated (arrows). Scale bars, 10 μm. (**J**) Decrease in LEC nuclear length in wild-type E11.5 mouse embryos, from which 10 nl (dark grey column) or 100 nl interstitial fluid (light grey column) was removed compared with untreated wild-type E11.5 mouse embryos (black column). All values are means ± s.d., $n=50$–200 cells per embryo in a total of three embryos per condition, $^*P<0.05$ (first bracket: $P=0.001$, second bracket: $P=0.002$). (**K**) Decrease in sites of VEGFR3 with phosphorylated tyrosines in LECs of wild-type E11.5 mouse embryos from which 10 nl (dark grey column) or 100 nl interstitial fluid (light grey column) was removed compared with untreated wild-type E11.5 mouse embryos (black column). All values are means ± s.d., $n=3$ embryos per condition, $^*P<0.05$ (first bracket: $P=0.008$, second bracket: $P=0.019$). (**L**) Decrease in LEC proliferation in wild-type E11.5 mouse embryos, from which 10 nl (dark grey column) or 100 nl interstitial fluid (light grey column) was removed compared with untreated wild-type E11.5 mouse embryos (black column). All values are means ± s.d., $n=3$ embryos per condition, $^*P<0.05$ (first bracket: $P=0.019$, second bracket: $P=0.04$).

when VEGF-C was injected compared with control injections (compare Supplementary Figure S1A and B with Supplementary Figure S1C and D and see Supplementary Figure S1E).

We also observed that LEC proliferation, as determined by the percentage of phospho-Histone H3-positive LEC nuclei, increased between E11.5 and E12.0 and decreased between E12.0 and E12.5 (compare Figure 1D and D′ with Figure 1H

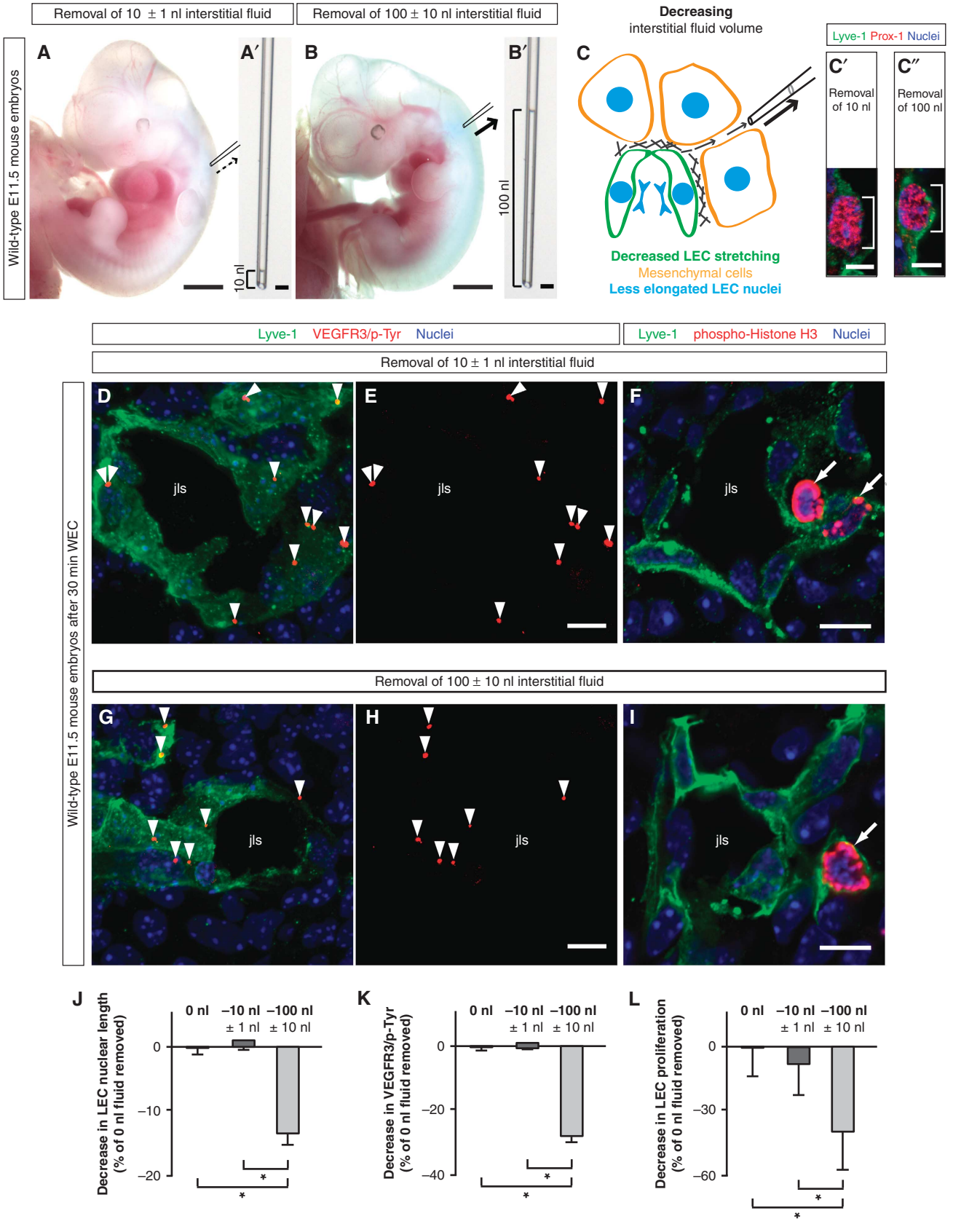

and H′, and see Figure 1L). Moreover, the jls profoundly increased in size from E11.5 to E12.0 (compare size of 'jls' in Figure 1C and D with Figure 1G and H). Thus, our data point to the following scenario: fluid accumulates within the jugular interstitium from E11.5 to E12.0, stretches the LECs, and induces LEC proliferation and growth of the lymphatic vasculature via VEGFR3 signalling. Subsequently, the expanded lymphatic vasculature drains the fluid, and the interstitial fluid volume decreases from E12.0 to E12.5. This reduces the LEC stretching and attenuates VEGFR3 signalling and proliferation, thus slowing down the growth of the primary lymphatic vasculature.

Reduction of VEGFR3 phosphorylation and LEC proliferation in 'loss-of-fluid' experiments

We next asked whether a decrease in interstitial fluid volume reduces LEC proliferation. To this end, we designed 'loss-of-fluid' experiments with the goal of removing extracellular fluid from the jugular interstitium (Figure 2). More specifically, we removed defined volumes of interstitial fluid from the jugular region of E11.5 mouse embryos (Figure 2A, A′, B, and B′). The aspirated fluid was then checked for the presence of cells to exclude the possibility that any cell was removed from the embryonic tissue (Supplementary Figure S2).

Decreasing the fluid volume within the jugular interstitium by 100 nl significantly reduced the lengths of LEC nuclei (Figure 2C, C′, C″, and J), suggesting that the cells were less stretched upon removal of interstitial fluid. In addition, the manipulated embryos were cultured for 30 min in whole embryo culture (WEC) as previously described (Strilić *et al*, 2009), and subsequently analysed for VEGFR3 tyrosine phosphorylation by PLA and for LEC proliferation by phospho-Histone H3 immunostaining. Aspiration of interstitial fluid was found to significantly reduce VEGFR3 phosphorylation, as indicated by the reduced number of PLA signals (compare Figure 2D and E with Figure 2G and H, and see Figure 2K). Moreover, LEC proliferation was also reduced (compare Figure 2F with Figure 2I, and see Figure 2L). The results from these 'loss-of-fluid' experiments show that lowering the interstitial fluid volume reduces LEC elongation, VEGFR3 tyrosine phosphorylation, and LEC proliferation in the lymphatic vasculature of the developing mouse embryo.

Enhanced VEGFR3 phosphorylation and LEC proliferation in 'gain-of-fluid' experiments

We next asked whether increasing the interstitial fluid volume enhances VEGFR3 phosphorylation and LEC proliferation. To this end, we injected different volumes of coloured PBS into the jugular region of developing E11.5 mouse embryos (Figure 3A and B). Importantly, LEC nuclei were found to be significantly more elongated upon injection of 34 nl PBS, compared with LEC nuclei of untreated mouse embryos or mouse embryos injected with only 4.2 nl PBS (Figure 3C, C′, C″, and J). In addition, injection of a large fluid volume increased tyrosine phosphorylation of VEGFR3 as indicated by the increased number of PLA signals (compare Figure 3D and E with Figure 3G and H, and see Figure 3K), and concomitantly increased LEC proliferation (compare Figure 3F and I, and see Figure 3L). To rule out the possibility that the injection of PBS induced LEC proliferation due to osmolar changes, we removed jugular interstitial fluid from embryos and injected it into others of the same age (Supplementary Figure S3). The data showed that injection of a large volume of interstitial fluid also increased LEC proliferation (compare Supplementary Figure S3A and B with Supplementary Figure S3C and D, and see Supplementary Figure S3E).

Since VEGFR3 homodimers and VEGFR3/2 heterodimers are found to be present in endothelial cells (Nilsson *et al*, 2010), we next examined the expression of VEGF receptors in LECs and VECs of the jugular area at E12.0 (Supplementary Figure S4). VEGFR3 is mainly expressed in LECs of the jls (compare Supplementary Figure S4I–K with Supplementary Figure S4L–N), whereas the expression of VEGFR2 is found both in LECs (Supplementary Figure S4C–E) and in VECs (Supplementary Figure S4F–H). Since VEGFR2, like VEGFR3, is expressed in LECs of the jls, we analysed VEGFR2 phosphorylation in LECs upon fluid injection (Supplementary Figure S5). Importantly, fluid injection did not result in an increased tyrosine phosphorylation of VEGFR2 (compare Supplementary Figure S5A and B with Supplementary Figure S5C and D, and see Supplementary Figure S5E), suggesting that fluid accumulation selectively activated VEGFR3 signalling in LECs (compare Supplementary Figure S5E with Figure 3K).

We also analysed the proliferation of VECs in the mouse embryos injected with PBS (Supplementary Figure S6). In contrast to LECs, the proliferation of VECs did not significantly change in response to an increased interstitial fluid volume (compare Supplementary Figure S6A and A′ with Supplementary Figure S6B and B′, and see Supplementary Figure S6C). The results from these 'gain-of-fluid' experiments show that an increase in the interstitial fluid volume increases LEC elongation and specifically enhances VEGFR3 tyrosine phosphorylation and cell proliferation in LECs.

'Loss-' and 'gain-of-fluid' experiments decrease and increase the numbers of LECs, respectively

To investigate whether fluid removal reduced the numbers of LECs, we cultivated aspirated embryos for 5 h in WEC and then quantified their LEC number (Figure 4). In these experiments, decreasing the fluid volume was found to reduce the number of LECs (compare Figure 4A with Figure 4B and see Figure 4C). Conversely, we showed that an increased amount of interstitial fluid resulted in an increased number of LECs after 5 h WEC (compare Figure 4D with Figure 4E and see Figure 4F). Therefore, the amount of interstitial fluid directly influences the number of LECs.

Increased β1 integrin activation in 'gain-of-fluid' experiments and upon mechanical stretching of LECs

To understand the molecular mechanism involved in our previous observations, we turned to integrins, which are known to act as mechanoreceptors (reviewed by Ingber, 2006 and Schwartz, 2010). β1 integrins were found to be expressed in the LECs of the jls (Supplementary Figure S4), and represent the largest subfamily of integrins. Moreover, some β1 integrins, such as α5β1 integrin, have been shown to be involved in mechanotransduction (reviewed by Ingber, 2006; Schwartz, 2010). β1 Integrins link the ECM with the actin cytoskeleton, thus connecting the extracellular environment with intracellular networks (reviewed by Ingber, 2006; Friedland *et al*, 2009; Schwartz, 2010). They have previously been shown to be involved in lymph valve formation *in vivo*

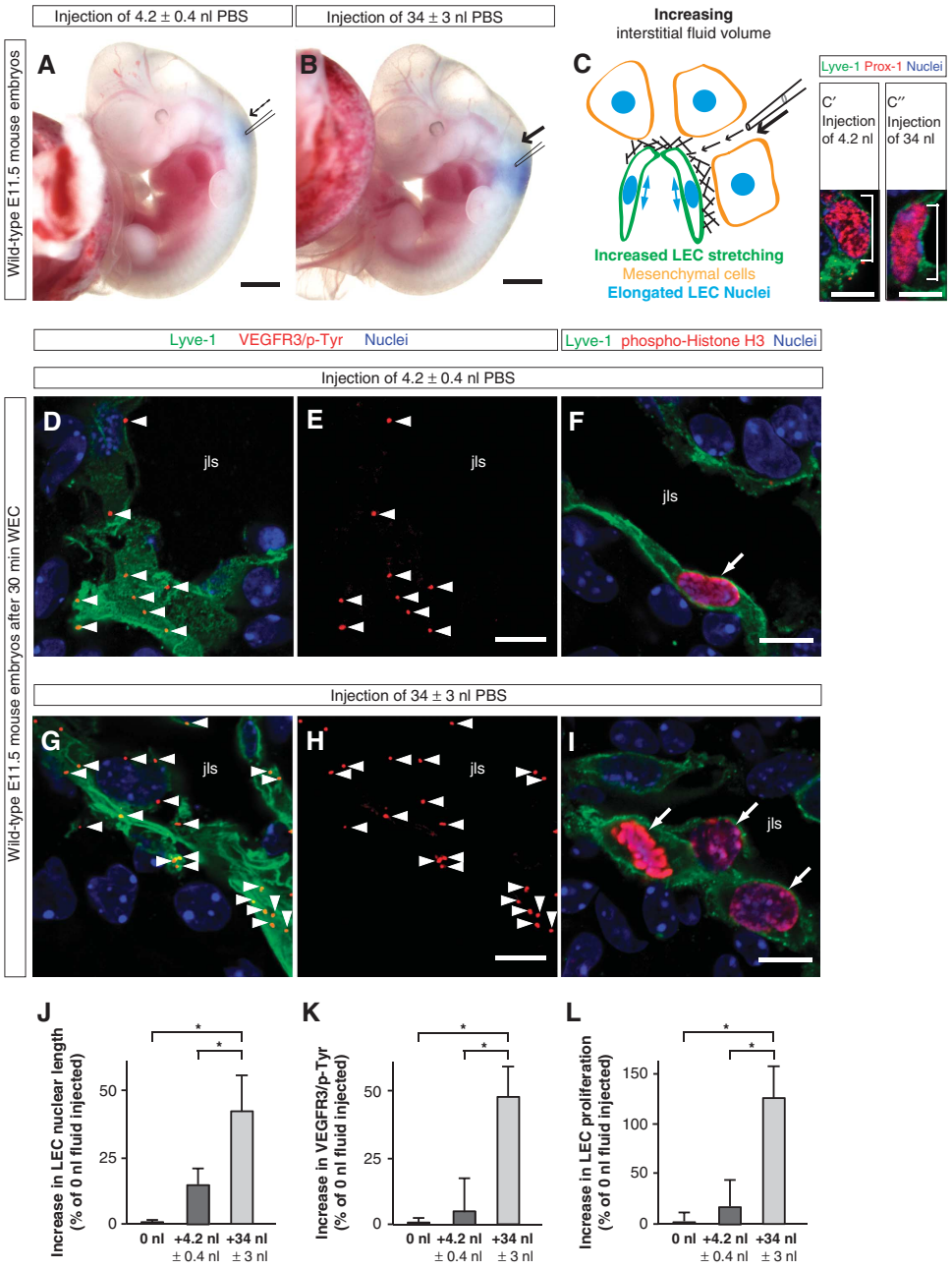

Figure 3 'Gain-of-fluid' experiments: Increasing the interstitial fluid volume elongates LECs, and enhances VEGFR3 tyrosine phosphorylation and LEC proliferation. (**A**, **B**) Representative bright field images of wild-type E11.5 mouse embryos in which (**A**) 4.2 nl PBS or (**B**) 34 nl PBS was injected together with Fast Green dye next to the jugular lymph sac. Scale bars, 1 mm. (**C**) Schematic illustration of the addition of fluid to embryonic tissue using a glass micro-capillary. When the interstitial fluid pressure is increased, the LECs are stretched, and their nuclei are elongated. (**C′**, **C″**) Laser scanning microscopy (LSM) images of LECs immunostained for Lyve-1 (green) and Prox-1 (red) to visualize the nuclear elongation when (**C″**) 34 nl interstitial fluid was injected compared with (**C′**) the injection of 4.2 nl interstitial fluid. Scale bars, 5 μm. (**D**, **E**, **G**, **H**) Representative LSM images of proximity ligation assays (PLA) on cross-sections through the jugular lymph sacs (jls) of wild-type E11.5 mouse embryos injected with (**D**, **E**) 4.2 nl PBS or (**G**, **H**) 34 nl PBS, and cultivated for 30 min in whole embryo culture (WEC). Red staining (arrowheads) indicates sites of VEGFR3 with phosphorylated tyrosines. A co-staining is shown for the lymphatic marker Lyve-1 (green) and nuclei (DAPI, blue). Scale bars, 10 μm. (**F**, **I**) Cross-sections through the jugular lymph sac (jls) of representative wild-type E11.5 mouse embryos injected with (**F**) 4.2 nl PBS or (**I**) 34 nl PBS, and immunostained for Lyve-1 (green), proliferation marker phospho-histone H3 (red) and nuclei (DAPI, blue). Proliferating cells are indicated (arrows). Scale bars, 10 μm. (**J**) Increase in LEC nuclear length in wild-type E11.5 mouse embryos injected with 4.2 nl PBS (dark grey column) or 34 nl PBS (light grey column) compared with untreated wild-type E11.5 mouse embryos (black column). All values are means ± s.d., $n = 20$–200 cells per embryo in a total of $\geqslant 3$ embryos per condition, $^*P < 0.05$ (first bracket: $P = 0.013$, second bracket: $P = 0.031$). (**K**) Increase in sites of VEGFR3 with phosphorylated tyrosines in LECs of wild-type E11.5 mouse embryos injected with 4.2 nl PBS (dark grey column) or 34 nl PBS (light grey column) compared with untreated wild-type E11.5 mouse embryos (black column). All values are means ± s.d., $n \geqslant 3$ embryos per condition, $^*P < 0.05$ (first bracket: $P = 0.0004$, second bracket: $P = 0.00009$). (**L**) Increase in LEC proliferation in wild-type E11.5 mouse embryos injected with 4.2 nl PBS (dark grey column) or 34 nl PBS (light grey column) compared with untreated wild-type E11.5 mouse embryos (black column). All values are means ± s.d., $n = 3$ embryos per condition, $^*P < 0.05$ (first bracket: $P = 0.032$, second bracket: $P = 0.025$).

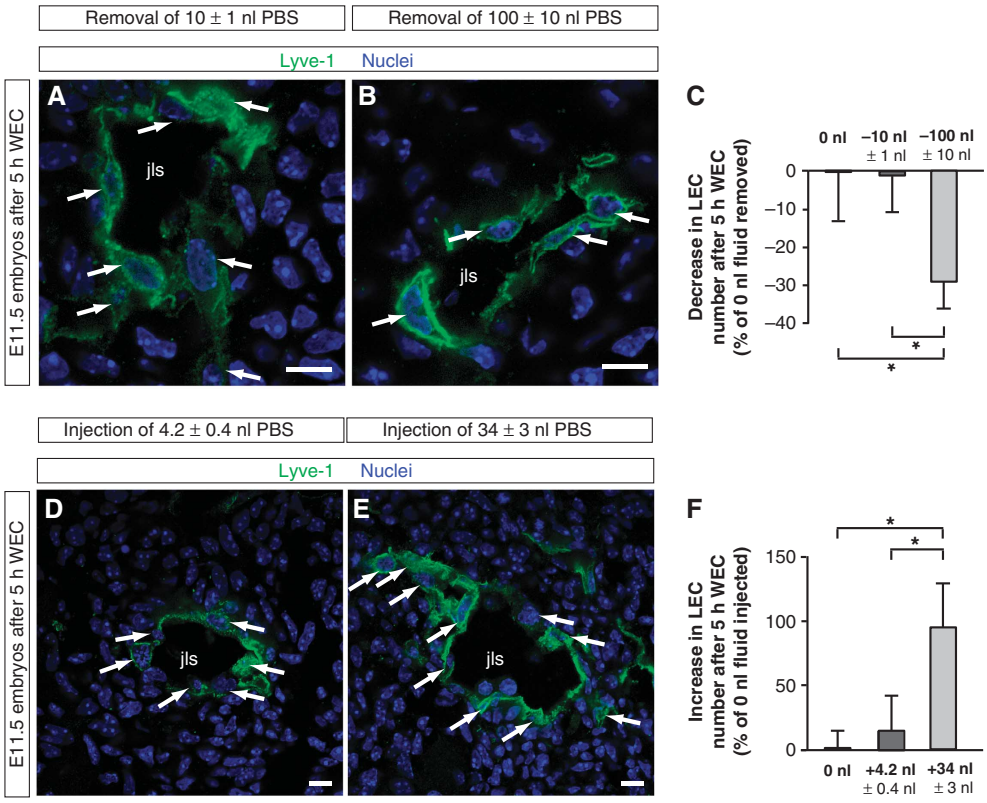

Figure 4 'Loss-' and 'gain-of-fluid' experiments: Lowering the interstitial fluid volume reduces the number of LECs, whereas increasing the interstitial fluid volume enhances their number. (**A**, **B**) Cross-sections through the jugular lymph sac (jls) of representative wild-type E11.5 mouse embryos, from which (**A**) 10 nl or (**B**) 100 nl interstitial fluid was removed. The embryos were subsequently cultivated for 5 h in WEC, and immunostained for Lyve-1 (green) and nuclei (DAPI, blue). Arrows point to LECs. Scale bars, 10 μm. (**C**) Decrease in LEC number in wild-type E11.5 mouse embryos, from which 10 nl (dark grey column) or 100 nl interstitial fluid (light grey column) was removed compared with untreated wild-type E11.5 mouse embryos (black column). All values are means ± s.d., $n = 3$ embryos per condition, $^*P < 0.05$ (first bracket: $P = 0.047$, second bracket: $P = 0.026$). (**D**, **E**) Cross-sections through the jugular lymph sac (jls) of representative wild-type E11.5 mouse embryos injected with (**D**) 4.2 nl PBS or (**E**) 34 nl PBS. The embryos were subsequently cultivated for 5 h in WEC, and immunostained for Lyve-1 (green) and nuclei (DAPI, blue). Arrows point to LECs. Scale bars, 10 μm. (**F**) Increase in LEC number in wild-type E11.5 mouse embryos injected with 4.2 nl PBS (dark grey column) or 34 nl PBS (light grey column) compared with untreated wild-type E11.5 mouse embryos (black column). All values are means ± s.d., $n \geqslant 3$ embryos per condition, $^*P < 0.05$ (first bracket: $P = 0.027$, second bracket: $P = 0.026$).

(Bazigou *et al*, 2009), and in lymphangiogenesis during various pathologies, such as inflammation, tumour growth, and wound healing (Hong *et al*, 2004; Kajiya *et al*, 2005; Chen *et al*, 2007; Dietrich *et al*, 2007; Okazaki *et al*, 2009; Garmy-Susini *et al*, 2010). In addition, α5β1 integrin was shown to associate with VEGFR3 and to trigger its activation via c-Src (Zhang *et al*, 2005; Galvagni *et al*, 2010). Moreover, a direct binding of VEGF-C to α9β1 integrin was reported (Vlahakis *et al*, 2005).

To test whether β1 integrins play a role in mechanotransduction of VEGFR3 signalling and LEC proliferation, we first investigated whether the activation state of β1 integrins changed in response to an increase in interstitial fluid volume. β1 Integrins were found to be significantly activated in LECs upon injection of a large fluid volume (34 nl) when compared with no injection (0 nl) or injection of a small fluid volume (4.2 nl) (compare Supplementary Figure S7A–C with Supplementary Figure S7E–G, and see Supplementary Figure S7M). Similarly, mechanical stretching of LECs increased β1 integrin activation (Supplementary Figure S8A–C). In addition, β1 integrins partially colocalized with VEGFR3 in response to both an increased interstitial fluid volume (compare Supplementary Figure S7D with Supplementary Figure S7H, and see Supplementary Figure S7N) and mechanical cell stretching (Supplementary Figure S8D–G). PLAs also indicated an increased interaction of VEGFR3 with β1 integrins following fluid accumulation (compare Supplementary Figure S7I and J with Figure S7K and L, and see Supplementary Figure S7O) and mechanical cell stretching (Supplementary Figure S8H–K). Furthermore, cell stretching led to the accumulation of β1 integrins and F-actin at focal sites of the plasma membrane (Supplementary Figure S8L–O). Our data therefore point to a mechanoinduced activation of β1 integrins and interaction of β1 integrins with VEGFR3.

Mechanical stretching of LECs enhances VEGFR3 tyrosine phosphorylation and LEC proliferation in a β1 integrin-dependent manner

Since VEGFR3 signalling and LEC proliferation correlate with LEC elongation *in vivo*, we next asked whether mechanical stretching increased VEGFR3 tyrosine phosphorylation and LEC proliferation *in vitro*. As shown by live-cell imaging of stretched and non-stretched LECs, the stretching resulted in an elongation of both cell body and nucleus of the LECs (Supplementary Figure S9A–D). Importantly, mechanical stretching and VEGF-C stimulation alone significantly increased both VEGFR3 tyrosine phosphorylation (Supplementary Figures S9E and S10) and LEC proliferation

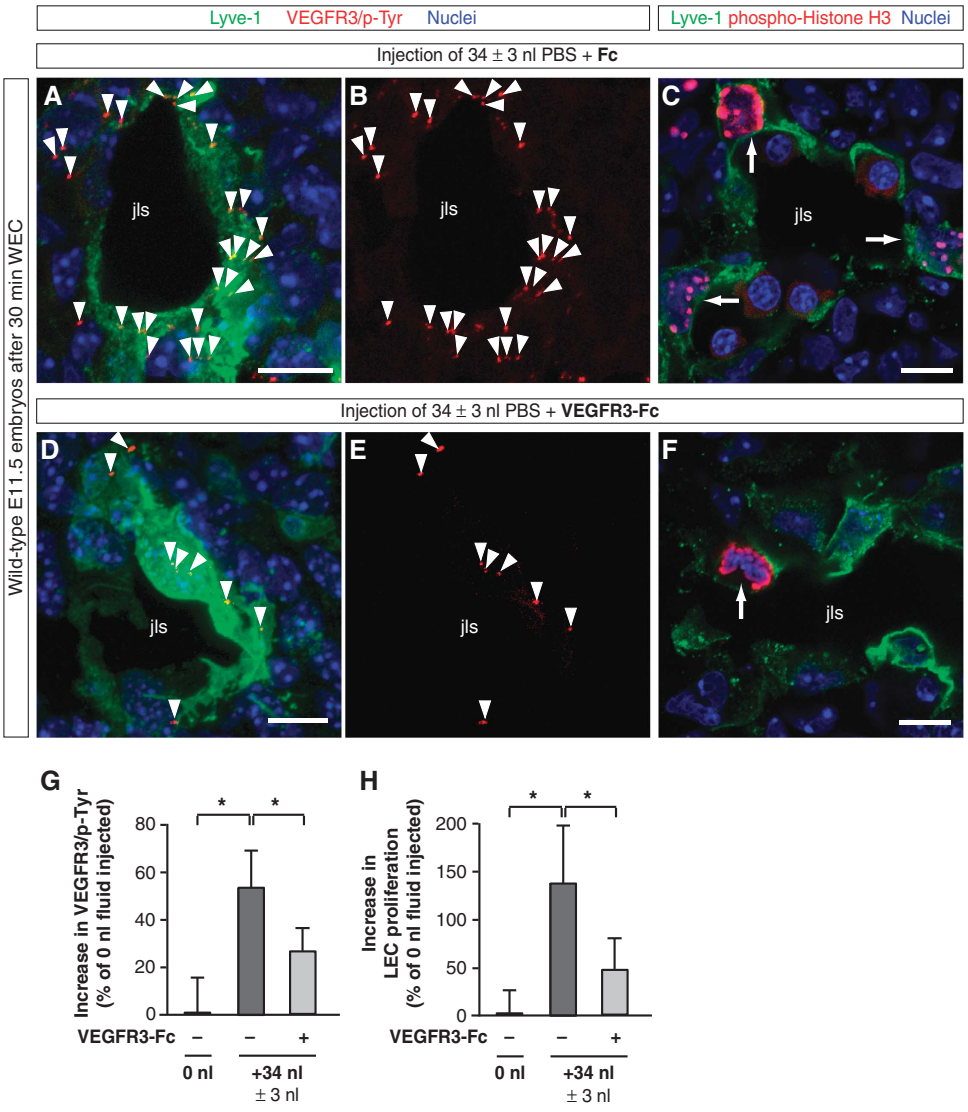

Figure 5 'Gain-of-fluid' experiments: VEGFR3-Fc reduces VEGFR3 tyrosine phosphorylation and LEC proliferation in response to an increased interstitial fluid volume. (**A**, **B**, **D**, **E**) Representative LSM images of proximity ligation assays (PLA) on cross-sections through jugular lymph sacs (jls) of wild-type E11.5 mouse embryos injected with (**A**, **B**) 34 nl PBS and control Fc protein or (**D**, **E**) 34 nl PBS and VEGFR3-Fc, and cultivated for 30 min in WEC. Red staining (arrowheads) indicates sites of VEGFR3 with phosphorylated tyrosines in LECs stained for Lyve-1 (green) and nuclei (DAPI, blue). Scale bars, 10 μm. (**C**, **F**) Cross-sections through jugular lymph sacs (jls) of representative wild-type E11.5 mouse embryos injected with (**C**) 34 nl PBS and control Fc protein or (**F**) 34 nl PBS and VEGFR3-Fc, and immunostained for Lyve-1 (green), proliferation marker phospho-histone H3 (red) and nuclei (DAPI, blue). Proliferating cells are indicated (arrows). Scale bars, 10 μm. (**G**) Increase in PLA sites of VEGFR3 with phosphorylated tyrosines in LECs of wild-type E11.5 mouse embryos injected with 34 nl PBS and control Fc protein (dark grey column) or 34 nl PBS and VEGFR3-Fc (light grey column) compared with untreated wild-type E11.5 mouse embryos (black column). All values are means ± s.d., $n \geqslant 3$ embryos per condition, $^*P < 0.05$ (first bracket: $P = 0.011$, second bracket: $P = 0.045$). (**H**) Increase in LEC proliferation in wild-type E11.5 mouse embryos injected with 34 nl PBS and control Fc protein (dark grey column) or 34 nl PBS and VEGFR3-Fc (light grey column) compared with untreated wild-type E11.5 mouse embryos (black column). All values are means ± s.d., $n \geqslant 3$ embryos per condition, $^*P < 0.05$ (first bracket: $P = 0.019$, second bracket: $P = 0.045$).

(Supplementary Figure S11). Moreover, the combination of mechanical stretching and VEGF-C stimulation led to a synergistic increase in LEC proliferation (Supplementary Figure S11E). To show that VEGFR3 signalling can also be mechanoinduced using a different experimental set-up (Tse and Engler, 2010), LECs were grown on substrates with increasing stiffness (Supplementary Figure S9F). Consistent with the notion of mechanoinduced VEGFR3 signalling, an increased stiffness also enhanced VEGFR3 tyrosine phosphorylation (Supplementary Figure S9F). Finally, stretching LECs did not increase the mRNA expression of VEGF-C (Supplementary Figure S12), suggesting that VEGFR3 can be mechanoinduced independent of changes in VEGF-C expression. Together, these results show that VEGFR3 signalling and LEC proliferation are subject to mechanotransduction.

We then investigated whether β1 integrins were required for translating mechanical stretching into VEGFR3 phosphorylation and LEC proliferation (Supplementary Figures S9 and S11). Using live-cell imaging, LECs and their nuclei were found to elongate upon mechanical stretching even when β1 integrins were silenced by 70–80% using two sets of siRNA molecules (compare Supplementary Figure S9B with

Supplementary Figure S9C, see Supplementary Figure S9D, and data not shown). However, VEGFR3 tyrosine phosphorylation and LEC proliferation only increased significantly when β1 integrins were present in LECs (Supplementary Figures S9E and S11). Finally, we showed that VEGFR3 signalling was required for LEC proliferation in response to fluid accumulation *in vivo* and cell stretching *in vitro* using VEGFR3-Fc and VEGFR3 siRNA, respectively (Figure 5; Supplementary Figure S11). These data demonstrate that β1 integrins are strictly required for increasing VEGFR3 tyrosine phosphorylation and for enhancing LEC proliferation via VEGFR3 in response to mechanical stretching.

β1 integrins are required for VEGFR3 tyrosine phosphorylation, LEC proliferation, and lymph vessel expansion in vivo

In previous studies, β1 integrin was deleted in blood vessels at different times of embryonic development. The consequences of gene deletion depended on the choice of promoter used to express Cre recombinase in endothelial cells (Carlson *et al*, 2008; Lei *et al*, 2008; Tanjore *et al*, 2008; Zovein *et al*, 2010). Here, we chose a fragment of the vascular endothelial growth factor receptor-2 (Vegfr2/Flk1) promoter to drive Cre recombinase in endothelial cells since the timing of its expression was optimal for deleting the β1 integrin in LECs (Supplementary Figure S13A–D; Licht *et al*, 2004, 2006). Using this promoter, we were able to efficiently remove the β1 integrin protein from LECs of the jls from E11.5 onwards, but not earlier (Supplementary Figure S13E–J and data not shown). In agreement with the immunohistochemistry data, LECs sorted from E12.0 to E12.5 β1 integrin-deficient embryos presented a reduction in the β1 integrin gene expression of around 75% compared with the LECs of heterozygous controls (Supplementary Figure S13K and L). Therefore, the β1 integrin was depleted to a large extent in LECs at the time when the jls started to expand in size (compare Supplementary Figure S13E–G with Supplementary Figure S13H–J). Using this Vegfr2/Flk1-Cre mouse, we observed haemorrhages and embryonic lethality (Figure 6E; Supplementary Figure S14A), a phenotype similar to that previously observed when β1 integrin was deleted using different endothelial cell-specific Cre mice (Carlson *et al*, 2008; Lei *et al*, 2008; Tanjore *et al*, 2008; Zovein *et al*, 2010). In addition, we observed dorsolateral oedema (compare Figure 6A with Figure 6E), which was reported only by one previous study that used a late endothelial cell-specific promoter (Zovein *et al*, 2010).

To date, lymphatic defects have not yet been investigated in mouse embryos deficient for β1 integrins in endothelial cells. Since large oedema on the back of the majority of mouse embryos pointed to lymphatic defects (Figure 6E; Supplementary Figure S14A), we analysed the LEC numbers, VEGFR3 tyrosine phosphorylation, and LEC proliferation in the jls at E12.0, shortly after the β1 integrin protein was lost in LECs.

Consistent with the timing of β1 integrin deletion, β1 integrin-deficient LECs were able to form jls, but the sacs were significantly smaller when compared with controls (compare Figure 6I–L with Figure 6M–P). In the absence of β1 integrin, VEGFR3 tyrosine phosphorylation (compare Figure 6B and C with Figure 6F and G and see Figure 6Q), LEC proliferation (compare Figure 6D with Figure 6H and see Figure 6R), and the numbers of LECs (Figure 6S) were significantly reduced. In contrast, the rate of apoptosis in LECs, as determined by caspase-3 immunostaining, differed neither at E11.5 nor at E12.5 (Supplementary Figure S15). Moreover, β1 integrin-deficient mice displayed a complete lack of dermal and mesenteric lymphatic vasculature at E15.5 of embryonic development (compare Supplementary Figure S14B–D with Supplementary Figure S14E–G). These data provide genetic evidence that β1 integrins are strictly required for lymph vessel expansion *in vivo*.

Reduced LEC numbers upon localized inhibition of β1 integrin activity in E11.5 mouse embryos

Since Vegfr2/Flk1-Cre mice delete β1 integrin in LECs as well as in VECs, we wished to rule out the possibility that the lymphatic defects were secondary to blood vascular defects. Thus, we injected β1 integrin function-blocking antibodies into the jugular region of E11.5 mouse embryos and cultured them for 12 h in WEC (Figure 7A and B; Supplementary Movie S2). This allowed us to block β1 integrins in the jugular region precisely at the onset of lymph vessel expansion.

Using this approach, we observed that the jls were significantly smaller in embryos injected with blocking

Figure 6 β1 integrin is required for interstitial fluid homeostasis and lymph vessel expansion. (**A**, **E**) Representative bright field images of the following mouse embryos: (**A**) β1 integrin$^{\Delta/+}$ control E13.5 embryo, containing a heterozygous deletion of β1 integrin in lymphatic endothelial cells (LECs) and (**E**) β1 integrin$^{\Delta/\Delta}$ E13.5 embryo, harbouring a homozygous deletion of β1 integrin in LECs. Arrows point to oedema in the dorsolateral part of the β1 integrin$^{\Delta/\Delta}$ embryo (**E**). Scale bars, 500 μm. (**B**, **C**, **F**, **G**) Representative LSM images of proximity ligation assays (PLA) on cross-sections through the jugular lymph sacs (jls) of β1 integrin$^{\Delta/+}$ control E12.0 mouse embryos (**B**, **C**) and β1 integrin$^{\Delta/\Delta}$ E12.0 embryos (**F**, **G**). Red staining (arrowheads) indicates the sites of VEGFR3 with phosphorylated tyrosines. A co-staining is shown for the lymphatic marker Lyve-1 (green) and nuclei (DAPI, blue). (**C**, **G**) Magnified areas of (**B**) and (**F**), respectively, showing only the PLA. Scale bars, 10 μm. (**D**, **H**) Cross-sections through the jugular lymph sac (jls) of (**D**) a representative β1 integrin$^{\Delta/+}$ control E12.0 mouse embryo and (**H**) a β1 integrin$^{\Delta/\Delta}$ E12.0 mouse embryo, immunostained for Lyve-1 (green), proliferation marker phospho-histone H3 (red) and nuclei (DAPI, blue). A proliferating cell is indicated (arrow). Scale bars, 20 μm. (**I**–**P**) Representative LSM images of cross-sections through (**I**–**L**) β1 integrin$^{\Delta/+}$ control embryos and (**M**–**P**) β1 integrin$^{\Delta/\Delta}$ embryos. The following stages of jugular lymph sac (jls) formation are shown: (**I**, **M**) E11.5, (**J**, **N**) E12.0, and (**K**, **L**, **O**, **P**) E12.5. Arrows point to the jugular lymph sacs (jls) stained for the lymphatic markers (**I**–**K**, **M**–**O**) Lyve-1 (green) or (**L**, **P**) Prox-1 (green), endothelial marker PECAM-1 (red) and nuclei (DAPI, blue). Anterior cardinal vein (acv) and dorsal aorta (da) are also indicated. Scale bars, 100 μm. (**Q**) Quantification of the sites of VEGFR3 with phosphorylated tyrosines in LECs of β1 integrin$^{\Delta/+}$ control E12.0 embryos (black column) and β1 integrin$^{\Delta/\Delta}$ E12.0 embryos (white column). All values are means ± s.d., $n = 3$ embryos per genotype, $^*P = 0.032$. (**R**) Quantification of the numbers of proliferating LECs in mouse embryos harbouring a heterozygous (black columns) or homozygous (white columns) deletion of β1 integrin. All values are means ± s.d., $n = 3$ embryos per genotype and stage, $^*P = 0.002$. (**S**) Quantification of the total numbers of LECs in mouse embryos harbouring a heterozygous (black columns) or homozygous (white columns) deletion of β1 integrin. All values are means ± s.d., $n \geqslant 4$ embryos per genotype and stage, $^*P < 0.05$ (first bracket: $P = 0.012$, second bracket: $P = 0.007$).

antibodies compared with embryos injected with isotype-matched control antibodies (compare Figure 7C with Figure 7D). In addition, the number of LECs was significantly reduced when β1 integrin function-blocking antibodies were injected (Figure 7E). Altogether our data show that β1 integrins are required in LECs for VEGFR3 phosphorylation, proliferation, and growth of the lymphatic vasculature.

β1 integrins are required for VEGFR3 tyrosine phosphorylation and LEC proliferation in response to an increased interstitial fluid volume

At E12.0 of mouse development, a rise in VEGFR3 signalling and LEC proliferation coincided with an increase in interstitial fluid pressure (compare Figure 1I with Figure 1K and L). However, this increase was not observed in the absence of β1 integrins

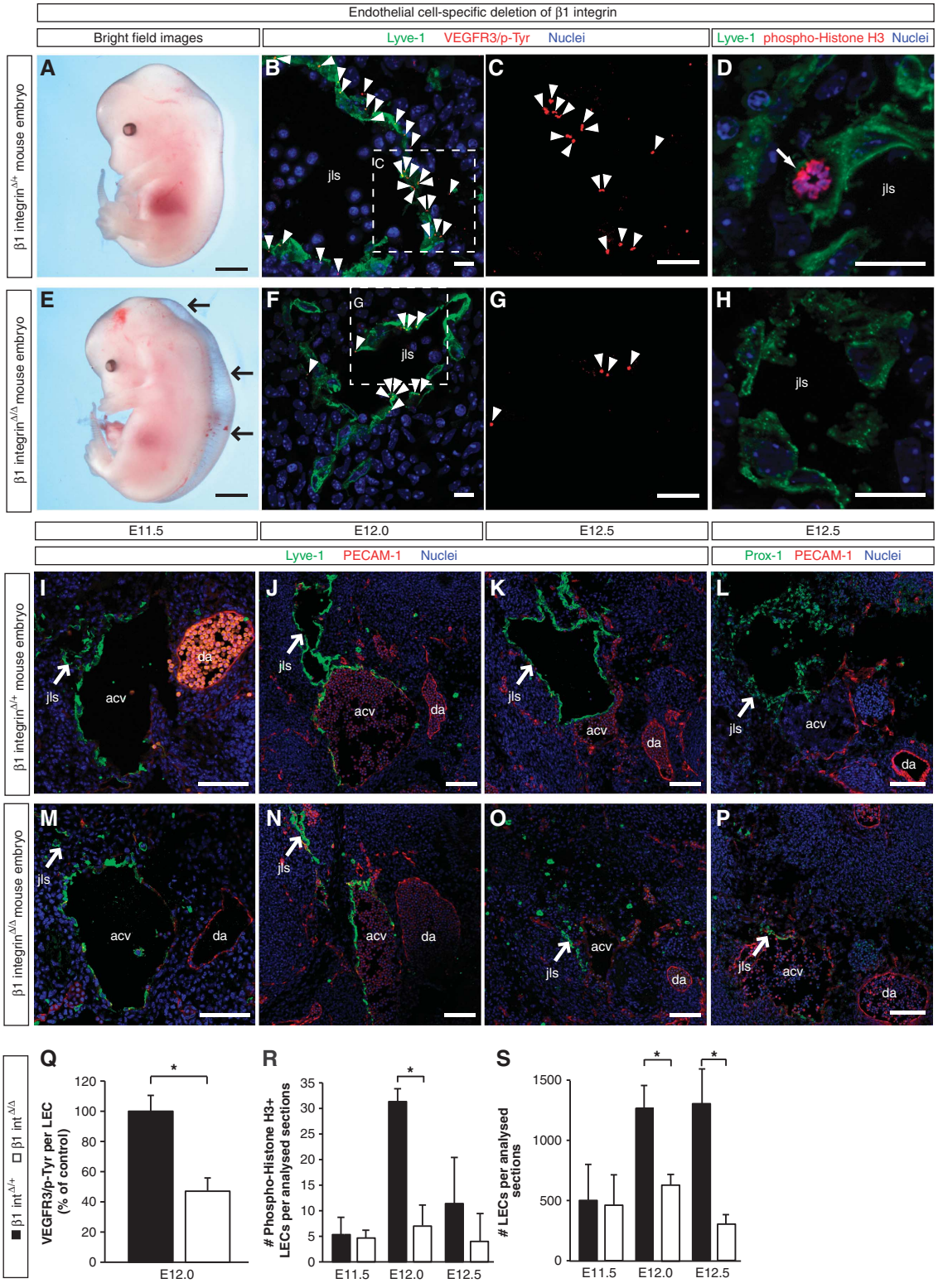

(Figure 6Q and R), suggesting that β1 integrins translated an increased interstitial fluid volume into enhanced VEGFR3 signalling and LEC proliferation. This notion was consistent with our finding that mechanical stretching of LECs only increased VEGFR3 signalling and LEC proliferation when β1 integrin was expressed (Supplementary Figures S9 and S11).

To directly investigate whether β1 integrin was required for fluid volume-induced VEGFR3 phosphorylation and LEC proliferation, 'gain-of-fluid' experiments were applied to mouse embryos in which β1 integrins were ablated in LECs (Figure 8). We observed that injection of PBS into the jugular region of β1 integrin-deficient E11.5 mouse embryos

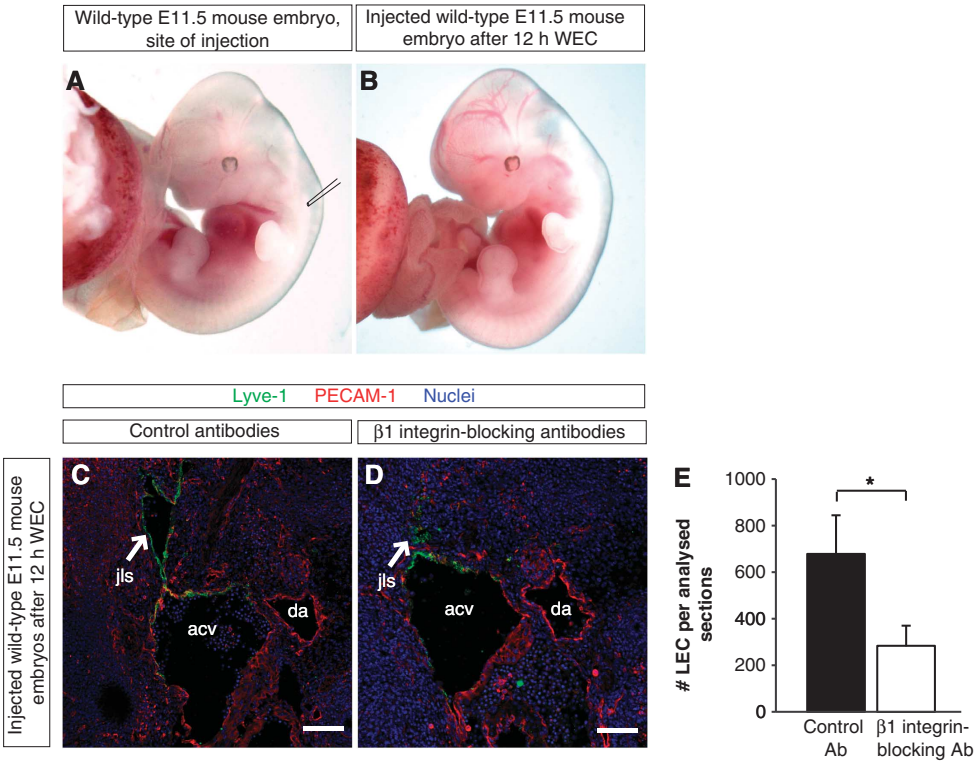

Figure 7 β1 integrin is required for lymph vessel expansion as revealed by injection of β1 integrin-blocking antibodies. (**A**, **B**) Bright field images of wild-type embryos isolated at E11.5 (**A**) before injection of antibodies and (**B**) after the injection and cultivation for 12 h in WEC. (**C**, **D**) Representative LSM images of cross-sections through wild-type E11.5 mouse embryos injected with (**C**) isotype-matched control antibodies or (**D**) with β1 integrin-blocking antibodies, and cultivated for 12 h in WEC. Arrows point to the jugular lymph sac (jls) stained for the lymphatic marker Lyve-1 (green), endothelial marker PECAM-1 (red), and nuclei (DAPI, blue). Anterior cardinal vein (acv) and dorsal aorta (da) are also indicated. Scale bars, 100 μm. (**E**) Quantification of the numbers of LECs in mouse embryos injected with isotype-matched control antibodies (black column) or with β1 integrin-blocking antibodies (white column). All values are means ± s.d., $n = 3$ mouse embryos per condition, $^*P = 0.008$.

Figure 8 'Gain-of-fluid' experiments: β1 integrin is required for VEGFR3 tyrosine phosphorylation and LEC proliferation in response to an increased interstitial fluid volume. (**A**, **B**, **D**, **E**) Representative LSM images of proximity ligation assays (PLA) on cross-sections through jugular lymph sacs (jls) of β1 integrin$^{\Delta/\Delta}$ E11.5 mouse embryos injected with (**A**, **B**) 4.2 nl PBS or (**D**, **E**) 34 nl PBS, and cultivated for 30 min in WEC. Red staining (arrowheads) indicates sites of VEGFR3 with phosphorylated tyrosines in LECs that are stained for Lyve-1 (green) and nuclei (DAPI, blue). Scale bars, 10 μm. (**C**, **F**) Cross-sections through the jugular lymph sac (jls) of representative β1 integrin$^{\Delta/\Delta}$ E11.5 mouse embryos injected with (**C**) 4.2 nl PBS or (**F**) 34 nl PBS, and immunostained for Lyve-1 (green), proliferation marker phospho-histone H3 (red), and nuclei (DAPI, blue). Proliferating cells are indicated (arrows). Scale bars, 10 μm. (**G**) Increase in LEC nuclear length in β1 integrin$^{\Delta/\Delta}$ E11.5 mouse embryos injected with 4.2 nl PBS (dark grey column) or 34 nl PBS (light grey column) compared with untreated β1 integrin$^{\Delta/\Delta}$ E11.5 mouse embryos (black column). All values are means ± s.d., $n = 50$–100 cells per embryo in a total of $\geqslant 3$ embryos per condition, $^*P < 0.05$ (first bracket: $P = 0.042$, second bracket: $P = 0.043$). (**H**) Lack of increase in sites of VEGFR3 with phosphorylated tyrosines in LECs of β1 integrin$^{\Delta/\Delta}$ E11.5 mouse embryos injected with 4.2 nl PBS (dark grey column) or 34 nl PBS (light grey column) compared with untreated β1 integrin$^{\Delta/\Delta}$ E11.5 mouse embryos (black column). All values are means ± s.d., $n \geqslant 3$ embryos per condition, NS, non-significant (first bracket: $P = 0.945$, second bracket: $P = 0.430$). (**I**) Lack of increase in LEC proliferation in β1 integrin$^{\Delta/\Delta}$ E11.5 mouse embryos injected with 4.2 nl PBS (dark grey column) or 34 nl PBS (light grey column) compared with untreated β1 integrin$^{\Delta/\Delta}$ E11.5 mouse embryos (black column). All values are means ± s.d., $n \geqslant 3$ embryos per condition, NS, non-significant (first bracket: $P = 0.651$, second bracket: $P = 0.688$). (**J**) Model: Interstitial fluid accumulation mechanoinduces lymph vessel expansion. An increase in interstitial fluid volume mechanically stretches LECs, enhances VEGFR3 tyrosine phosphorylation, and induces LEC proliferation. These steps strictly require β1 integrin. Both VEGF-C and β1 integrin induce VEGFR3 tyrosine phosphorylation, the latter possibly via the Src Family of Kinases (SFK) (data not shown) (Galvagni *et al*, 2010). The newly formed lymph vessels drain the interstitial fluid, thereby decreasing the interstitial fluid pressure, and preventing formation of oedema.

increased neither VEGFR3 tyrosine phosphorylation (compare Figure 8A and B with Figure 8D and E, and see Figure 8H) nor LEC proliferation (compare Figure 8C with Figure 8F, and see Figure 8I). In contrast, the LECs became elongated upon PBS injection (Figure 8G).

Based on these experiments, we propose that LECs are mechanically stretched when the interstitial fluid volume increases, and that β1 integrins are required for translating this mechanical signal into enhanced VEGFR3 signalling and LEC proliferation (Figure 8J).

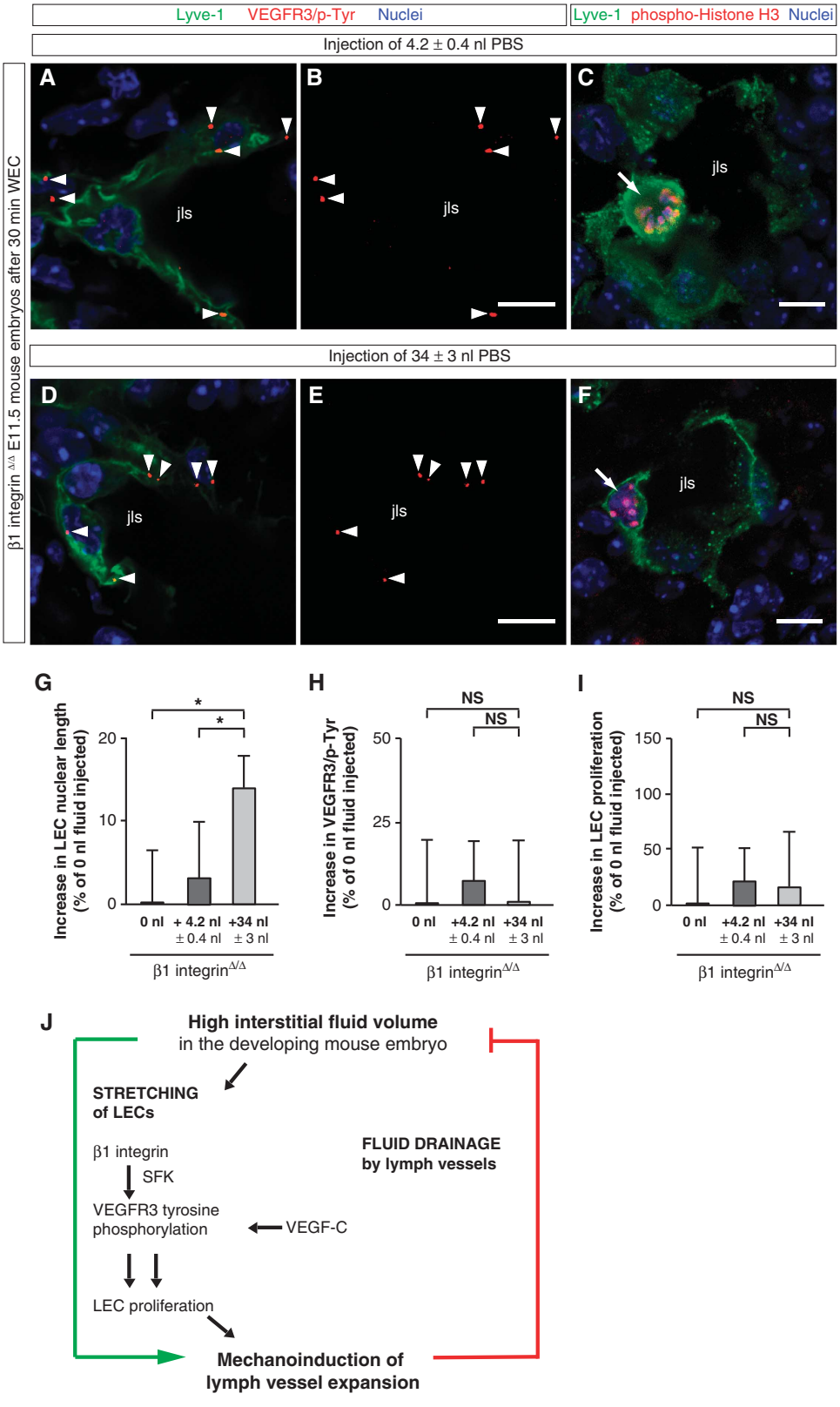

'Gain-of-fluid' experiments enhance LEC proliferation in sprouting and adult lymph vessels

To investigate whether β1 integrins were required for inducing LEC proliferation in sprouting lymph vessels in response to fluid accumulation, we applied 'gain-of-fluid' experiments to the dorsal skin of E15.5 mouse embryos along with either β1 integrin-blocking or control antibodies (Figure 9A–D). Injection of 100 nl PBS together with isotype-matched control antibodies induced LEC proliferation in dermal sprouting lymph vessels (compare Figure 9A with Figure 9B and see Figure 9D, first bracket). In contrast, blocking β1 integrins inhibited this enhanced LEC proliferation (compare Figure 9B with Figure 9C and see Figure 9D, second bracket).

Finally, injection of PBS into the ears of adult mice (compare Figure 9E with Figure 9I) also increased VEGFR3 phosphorylation in LECs (compare Figure 9F and G with Figure 9J and K, and see Figure 9M) and enhanced their proliferation (compare Figure 9H with Figure 9L, and see Figure 9N). In summary, our data suggest that interstitial fluid accumulation triggers LEC proliferation at different stages of lymphatic development and fluid homeostasis.

Discussion

Here, we have shown that cell proliferation in the developing lymphatic vasculature is correlated with the amount of fluid in the interstitium. An increase in fluid pressure between E11.5 and E12.0 of mouse embryonic development is associated with an increase in the proliferation rates of LECs. Conversely, when the fluid pressure decreases between E12.0 and E12.5, possibly due to fluid drainage via the expanded lymphatic vasculature, the proliferation rates of LECs decline. Since LECs elongate when the fluid pressure increases, our data suggest that an increase in the amount of interstitial fluid stretches the LECs, and that this stretching is a mechanical signal that contributes to lymph vessel expansion (Figure 8J). Applying a novel set of 'loss-of-fluid' and 'gain-of-fluid' experiments to the mouse embryos, we further demonstrated that LEC elongation, proliferation, and cell number changed in response to the amount of fluid present within the interstitium. We also showed that mechanical stretching of LECs significantly increased their proliferation.

Several mouse embryos deficient for genes involved in lymph vessel formation have been shown to develop lymph oedema as early as E12.5 of embryonic development (Karkkainen *et al*, 2004; Fritz-Six *et al*, 2008; D'Amico *et al*, 2010), showing dysfunctional fluid drainage at E12.5 when the early lymphatic vasculature is defective. Therefore, our hypothesis that the expanding lymphatic vasculature starts to drain fluid and thereby lowers the interstitial fluid pressure from E12.5 onwards is fully consistent with the timing of lymph oedema formation in these gene-deficient mouse embryos.

After showing that the amount of interstitial fluid influences LEC proliferation and lymph vessel growth, we started to investigate the underlying molecular mechanism. Mechanical strain has been reported to distort interconnected ECM scaffolds, which in turn produce cytoskeletal and nuclear changes in endothelial cells (reviewed by Ingber, 2006). Importantly, integrins that link the ECM to the actin cytoskeleton provide a means to distribute local forces from cell–ECM adhesions to distant sites in the cytosol and nucleus (reviewed by Geiger *et al*, 2009). Mechanical forces can therefore affect the entire cell via integrin-mediated signalling (reviewed by Ingber, 2006; Papusheva and Heisenberg, 2010; Schwartz, 2010). The largest subgroup of heterodimeric integrins is that containing the β1 integrin, and several β1 integrins have been reported to participate in lymphatic development in the adult or late embryonic mouse (Hong *et al*, 2004; Kajiya *et al*, 2005; Chen *et al*, 2007; Dietrich *et al*, 2007; Bazigou *et al*, 2009; Okazaki *et al*, 2009; Garmy-Susini *et al*, 2010). In addition, α5β1 integrins have been shown to exist in a complex with VEGFR3 (Zhang *et al*, 2005) and Tie2 (Cascone *et al*, 2005), thereby regulating endothelial cell responses to ECM and growth factors.

A role of β1 integrins in LEC proliferation and growth of the embryonic lymphatic vasculature, however, has not yet been reported. By using two independent experimental approaches, we unambiguously demonstrated that β1 integrins were strictly required for embryonic lymph vessel expansion. In addition, we provided genetic and pharmacological evidence that β1 integrins and VEGFR3 were needed for the proliferative response of LECs to both an increased interstitial fluid volume *in vivo* and mechanical stretching *in vitro*. Moreover, β1 integrins were necessary both *in vitro* and *in vivo* for the mechanoinduction of VEGFR3 signalling.

Figure 9 'Gain-of-fluid' experiments: Increasing the interstitial fluid volume enhances LEC proliferation in sprouting lymph vessels in a β1 integrin-dependent manner, and enhances VEGFR3 tyrosine phosphorylation and LEC proliferation in adult lymph vessels. (**A**–**C**) Skin of E15.5 mouse embryos injected with (**A**) 0 nl PBS and isotype-matched control antibodies, (**B**) 100 nl PBS and isotype-matched control antibodies, and (**C**) 100 nl PBS with β1 integrin-blocking antibodies, and whole-mount immunostained for Lyve-1 (green), proliferation marker phospho-histone H3 (red), and nuclei (DAPI, blue). Scale bars, 20 μm. (**A′**–**C′**) Magnification of (**A**–**C**). Scale bars, 10 μm. (**D**) Increase in LEC proliferation in the skin of E15.5 mouse embryos injected with 100 nl PBS and isotype-matched control antibodies (dark grey column) or 100 nl PBS and β1 integrin-blocking antibodies (light grey column) compared with control embryos (black column). All values are means ± s.d., $n = 3$ mouse embryos per condition, $^*P < 0.05$ (first bracket: $P = 0.019$, second bracket: $P = 0.049$). (**E**, **I**) Bright field images and schematic illustrations of mouse ears injected with (**E**) 10 μl PBS or (**I**) 100 μl PBS together with Fast Green dye. (**F**, **G**, **J**, **K**) Representative LSM images of proximity ligation assays (PLA) on cross-sections through mouse ears injected with (**F**, **G**) 10 μl PBS or (**J**, **K**) 100 μl PBS, and collected after 30 min. Red staining (arrowheads) indicates sites of VEGFR3 with phosphorylated tyrosines in LECs that are co-stained for Lyve-1 (green) and nuclei (DAPI, blue). Scale bars, 10 μm. (**H**, **L**) Cross-sections through mouse ears injected with (**H**) 10 μl PBS or (**L**) 100 μl PBS, and whole-mount immunostained for Lyve-1 (green), PECAM-1 (red), and proliferation marker phospho-histone H3 (grey). Proliferating cells are indicated (arrows). Scale bars, 50 μm. (**M**) Increase in sites of VEGFR3 with phosphorylated tyrosines in LECs of mouse ears injected with 10 μl PBS (dark grey column) or 100 μl PBS (light grey column) compared with untreated ears (black column). All values are means ± s.d., $n \geqslant 3$ mouse ears per condition, $^*P < 0.05$ (first bracket: $P = 0.0004$, second bracket: $P = 0.022$). (**N**) Increase in LEC proliferation in mouse ears injected with 10 μl PBS (dark grey column) or 100 μl PBS (light grey column) compared with untreated ears (black column). All values are means ± s.d., $n \geqslant 3$ mouse ears per condition, $^*P < 0.05$ (first bracket: $P = 0.003$, second bracket: $P = 0.002$).

In contrast, β1 integrins were required neither for the ability of LECs to be elongated by stretch or fluid accumulation nor for cell survival during early lymphatic development.

Our finding that LECs use β1 integrins to respond to an increased amount of fluid in the surrounding interstitium *in vivo* significantly advances previous cell culture

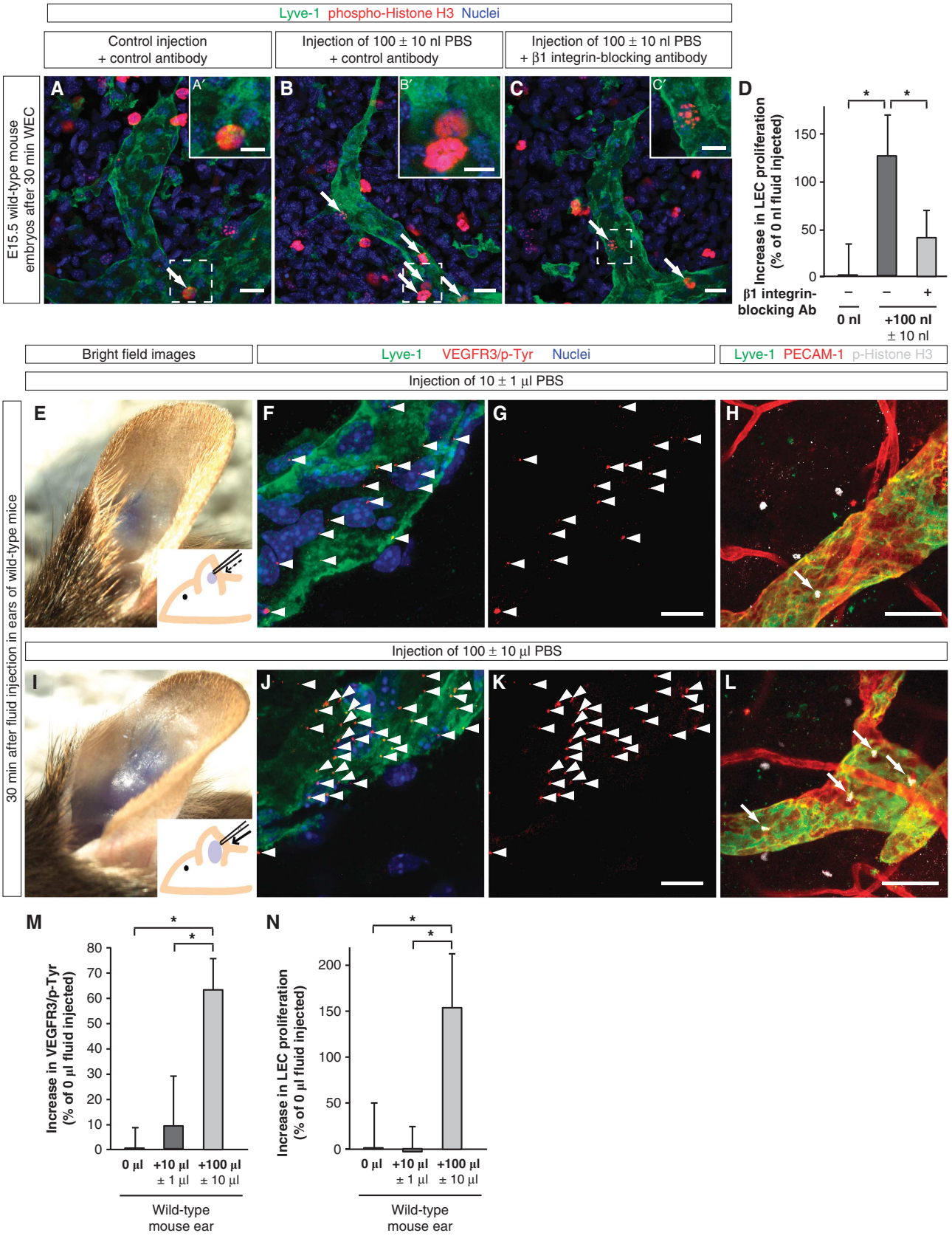

experiments showing that ECM proteins enhance VEGFR3 tyrosine phosphorylation and cell proliferation via β1 integrins *in vitro* (Zhang *et al*, 2005; Galvagni *et al*, 2010). Moreover, it was shown that β1 integrins activate Src Family Kinases (SFKs; Klinghoffer *et al*, 1999), which in turn phosphorylate VEGFR3 at tyrosine residues that are different from the residues phosphorylated by VEGF-C binding to VEGFR3 (Galvagni *et al*, 2010). Thus, SFKs are likely to be involved in the tyrosine phosphorylation of VEGFR3 that occurs in response to fluid accumulation and cell stretching (Figure 8J). In this regard, it is noteworthy that local mechanical stimulation of integrins can trigger long-range propagation of c-Src activation (Wang *et al*, 2005), indicating that the stretching of LECs might induce tyrosine phosphorylation of VEGF receptors that are not in close proximity to the mechanically activated β1 integrins. Whereas different aspects of VEGFR3 signalling have been recently reported (Siekmann and Lawson, 2007; Tammela *et al*, 2008; Machnik *et al*, 2009; Nilsson *et al*, 2010; Saharinen *et al*, 2010; Wang *et al*, 2010; Calvo *et al*, 2011), our results provide the first example of a mechanically driven and physiologically relevant activation of VEGFR3.

Combining our findings with published data, we now propose a model for how the size of the lymphatic vasculature is regulated in the developing mouse embryo (Figure 8J): an increasing amount of interstitial fluid changes the ECM scaffolds adjacent to LECs, so that these become stretched. This stretching activates β1 integrins on the LECs, which subsequently activate SFKs that propagate within the cells and tyrosine phosphorylate VEGFR3. The combined action of VEGF-C and mechanical stretching synergistically activates VEGFR3 signalling and LEC proliferation. Since the expanded lymphatic vasculature has an improved ability to drain fluid, the fluid pressure in the surrounding tissue decreases. This negative feedback reduces any further lymph vessel growth and might ensure that the lymphatic vasculature is appropriately sized to meet the tissue demand for fluid drainage. Since fluid injection into the embryonic mouse skin and the adult mouse ear also increased VEGFR3 tyrosine phosphorylation plus LEC proliferation (Figure 9), the mechanism proposed might broadly apply to lymph vessels in general.

Materials and methods

Mouse strains

C57Bl/6J mice were used for wild-type studies. Flk1-Cre mice, β1 integrin-loxP mice, and Rosa26R LacZ mice have been previously described (Soriano, 1999; Potocnik *et al*, 2000; Licht *et al*, 2004). Littermates, or mouse embryos of a similar genetic background, were used as controls. Pregnancies were dated by the presence of a vaginal plug (embryonic day (E) 0.5). Animal experiments were conducted and approved according to the German Animal Protection Laws.

Mouse embryo isolation, injections, and WEC

Mouse embryos were isolated at different embryonic stages. After isolation or WEC, embryos were fixed in 4% paraformaldehyde (PFA) or in 5% trichloroacetic acid (TCA), and processed for immunohistochemistry and imaging. For WEC, interstitial fluid was removed using a micro-injector Cell Tram Vario (Eppendorf), or substances were injected in PBS containing Fast Green dye (Sigma) using a Pneumatic PicoPump (World Precision Instruments). 100 μg/ml isotype-matched control antibody (BD Bioscience), 100 μg/ml β1 integrin-blocking antibody (BD Bioscience), 10 μg/ml VEGFR3-Fc chimera (Sigma), 10 μg/ml Fc protein control (Sigma), 500 ng/ml VEGF-C C156S (R&D Systems) or different volumes of PBS were injected next to the jls of mouse embryos. After fluid injection or fluid removal, the embryos were roller cultured (WEC) for the indicated times. The removed interstitial fluid was analysed for the presence of cells by briefly incubating it with Hoechst 3342 (Thermo Scientific).

Interstitial fluid pressure assessment

A glass micro-capillary (Harvard apparatus) was inserted in wild-type mouse embryos at different embryonic stages, and the amount of interstitial fluid that entered the micro-capillary was measured.

Immunostaining and imaging

For laser scanning microscopy (LSM), fixed embryos were cryopreserved in 30% sucrose (Sigma), embedded in O.C.T. embedding media (Fisher Scientific), and 12 μm cryo-sections were made. The following antibodies were used: goat anti-mouse Lyve-1 (R&D Systems AF2125), rat anti-mouse PECAM-1 (BD Bioscience 553370), rabbit anti-phospho-histone H3 (Millipore 06-570), rabbit anti-β-galactosidase (Sigma C8487), goat anti-Prox-1 (R&D Systems AF2727), rat anti-mouse β1 integrin clone MB1.2 (Millipore MAB1997), rabbit anti-activated Caspase-3 (Sigma C8487), rat anti-activated mouse β1 integrin clone 9EG7 (BD Bioscience 553715), goat anti-mouse VEGFR3 (R&D Systems AF743), rabbit anti-mouse VEGFR2 clone 55B11 (Cell Signaling 2479), and mouse anti-BrdU (BD Bioscience 555627). DAPI (Sigma) was used to stain cell nuclei. Secondary antibodies conjugated with AF488 or AF555 (Molecular Probes), Cy3 or Cy5 (Jackson ImmunoResearch) were used. LSM images were acquired using a Zeiss 510 LSM or a Zeiss 710 LSM. All images were analysed using Fiji/ImageJ image analysis software (http://pacific.mpi-cbg.de). Bright field images were captured using a Nikon SMZ1500 microscope and a Digital Sight DS-Fi1 camera. Colocalization analyses were performed using the colocalization plug-ins in Fiji/ImageJ. The analysis of activated β1 integrin in LECs was performed automatically using this Fiji/ImageJ image analysis software. A threshold mask of the staining for VEGFR3 was made and superimposed on the activated β1 integrin channel. The staining intensity in the specified region was subsequently quantified. For DAB peroxidase staining, HRP-coupled secondary antibodies (Invitrogen) and DAB substrate kit (Vector Lab) were used.

Proximity ligation assays

PLAs were performed on embryonic or ear mouse sections and on human LECs according to the manufacturer's protocol using the Duolink II Detection Kit (Olink Bioscience). The following antibodies were used: goat anti-mouse VEGFR3 (R&D Systems AF743), goat anti-human VEGFR3 (R&D Systems AF349), mouse anti-phospho-tyrosine 4G10 Platinum (Millipore 05-1050), rat anti-mouse β1 integrin clone MB1.2 (Millipore MAB1997), mouse anti-human β1 integrin clone P4C10 (Millipore MAB1987), and rabbit anti-mouse VEGFR2 clone 55B11 (Cell Signaling 2479). A co-staining was performed using rabbit anti-mouse Lyve-1 (Abcam ab14917) and goat anti-mouse Lyve-1 (R&D Systems AF2125). DAPI (Sigma) was used to stain cell nuclei. LSM images were acquired using a Zeiss 710 LSM. VEGFR3/p-Tyr, VEGFR2/p-Tyr, and VEGFR3/β1 integrin PLAs were quantified as the number of positive staining (total number of red dots) divided by the total number of Lyve-1-positive LECs.

In vitro studies

Human dermal microvascular LECs (Lonza) were grown in EGM-2MV medium (Lonza) and used at passages $<$P6 in all *in vitro* studies. Cells were grown on STREX stretch chambers (BioCat) coated with 2.5 μg/cm^2 fibronectin (BD Bioscience). Cells were transfected with 3 μg control esiRNA molecules against *Renilla reniformis* luciferase (RLuc), esiRNA molecules directed against β1 integrins, EGFP-β1 integrin vector for β1 integrin rescue experiments, esiRNA molecules directed against VEGFR3, or VEGFR3 vector for VEGFR3 rescue experiments, and were grown for 48 h. Subsequently, cells were starved, stimulated with 100 ng/ml VEGF-C (R&D Systems) and/or unidirectionally stretched with a STREX Mechanical Cell Strain Manual Stretcher (BioCat). For immunocytochemistry, cells were fixed with 4% PFA and immunostained with mouse anti-human β1 integrin clone P4C10 (Millipore MAB1987), goat anti-human VEGFR3 (R&D Systems AF349), and Phalloidin-Rhodamin (Invitrogen R415) antibodies. For the analysis of cell proliferation, cells were incubated with 10 μM BrdU (5-bromo-2′-deoxyuridine, Sigma), immediately washed, fixed in ethanol

fixative, and kept in PBS at 4°C until staining was performed. To measure VEGFR3 tyrosine phosphorylation, the cells were lysed in ice-cold lysis buffer (50 mM Hepes pH 7.0, 150 mM NaCl, 10% Glycerol, 1% Triton X-100, 1 mM Na_3VO_4, a complete cocktail of protease inhibitors (Roche)), centrifuged, and the supernatants were analysed using the DuoSet IC human phospho-VEGFR3 ELISA (R&D Systems). Differential interference contrast (DIC) images of living non-stretched and stretched LECs were captured using a Zeiss 710 LSM, and blind quantification of cell length was performed.

Preparation of polyacrylamide gels

Polyacrylamide gels were prepared with varying stiffness as previously described (Tse and Engler, 2010), and subsequently functionalized with 0.2 mg/ml sulfo-SANPAH (sulfosuccinimidyl-6-(4′-azido-2′-nitrophenylamino)-hexanoate; Thermo Fisher Scientific) and conjugated with 10 μg/ml fibronectin (BD Bioscience).

Real-time RT–PCR and RT–PCR analyses

For the assessment of vegf-c and β1 integrin mRNA expression, the cells were homogenized with peqGold TriFast (Peqlab). 1–2 μg total RNA was used for every RT–PCR experiment. For real-time RT–PCR, each sample was run in triplicate, and data were analysed according to the threshold cycle method (Stratagene). For RT–PCR experiments, agarose gels were run with the PCR products. β-actin and β2-microglobulin were used as internal controls. The following primers were used: human Vegf-c forward 5′-gggaagaagttccaccatca-3′, human Vegf-c reverse 5′-atgtggccttttccaatacg-3′, human β-actin forward 5′-acccagatcatgtttgagac-3′, human β-actin reverse 5′-gtca ggatcttcatgaggtagt-3′, mouse β1 integrin forward 5′-aatgccaagtggga cacggg-3′, mouse β1 integrin reverse 5′-tgactaagatgctgctgctgtgagc-3′, mouse β2-microglobulin forward 5′-gagcccaagaccgtctactg-3′, mouse β2-microglobulin reverse 5′-gctatttctttctgcgtgcat-3′.

Magnetic-activated cell sorting (MACS)

Mouse embryos were isolated and directly dissociated using the gentleMACS dissociator (Milteny Biotec). The cell suspensions were labelled with rat anti-mouse PECAM-1-FITC clone 390 (Millipore CBL1337F) and rabbit anti-mouse Lyve-1 (Abcam ab14917) antibodies. The LECs were sorted in a stepwise manner using first anti-FITC MultiSort microbeads (Milteny Biotec) and, second, goat anti-rabbit IgG microbeads (Milteny Biotec).

Statistical analysis

Statistical significance was determined using an unpaired two-tailed Student's *t*-test. Differences were considered significant with a *P*-value <0.05. Quantified data are presented as mean values ± s.d. or ± s.e.m. (see figure legends).

Supplementary data

Supplementary data are available at *The EMBO Journal* Online (http://www.embojournal.org).

Acknowledgements

We thank all our colleagues in Düsseldorf for helpful suggestions. The Deutsche Forschungsgemeinschaft (DFG LA1216/5-1) supported this study.

Author contributions: LPP and EL conceived and designed the project. BS initiated the project, whereas LPP performed most of the experiments. LPP and EL wrote the manuscript with input from BS, AG, GB, and RF. GB and RF provided mouse lines.

Conflict of interest

The authors declare that they have no conflict of interest.

References

Affolter M, Zeller R, Caussinus E (2009) Tissue remodelling through branching morphogenesis. *Nat Rev Mol Cell Biol* **10:** 831–842

Bahram F, Claesson-Welsh L (2010) VEGF-mediated signal transduction in lymphatic endothelial cells. *Pathophysiology* **17:** 253–261

Bazigou E, Xie S, Chen C, Weston A, Miura N, Sorokin L, Adams R, Muro AF, Sheppard D, Makinen T (2009) Integrin-alpha9 is required for fibronectin matrix assembly during lymphatic valve morphogenesis. *Dev Cell* **17:** 175–186

Calvo CF, Fontaine RH, Soueid J, Tammela T, Makinen T, Alfaro-Cervello C, Bonnaud F, Miguez A, Benhaim L, Xu Y, Barallobre MJ, Moutkine I, Lyytikkä J, Tatlisumak T, Pytowski B, Zalc B, Richardson W, Kessaris N, Garcia-Verdugo JM, Alitalo K *et al* (2011) Vascular endothelial growth factor receptor 3 directly regulates murine neurogenesis. *Genes Dev* **25:** 831–844

Carlson TR, Hu H, Braren R, Kim YH, Wang RA (2008) Cell-autonomous requirement for beta1 integrin in endothelial cell adhesion, migration and survival during angiogenesis in mice. *Development* **135:** 2193–2202

Cascone I, Napione L, Maniero F, Serini G, Bussolini F (2005) Stable interaction between α5β1 integrin and Tie2 tyrosine kinase receptor regulates endothelial cell response to Ang-1. *J Cell Biol* **170:** 993–1004

Chen L, Hug S, Gardner H, de Fougerolles AR, Barabino S, Dana MR (2007) Very late antigen 1 blockade markedly promotes survival of corneal allografts. *Arch Ophthalmol* **125:** 783–788

D'Amico G, Korhonen EA, Waltari M, Saharinen P, Laakkonen P, Alitalo K (2010) Loss of endothelial Tie1 receptor impairs lymphatic vessel development-brief report. *Arterioscler Thromb Vasc Biol* **30:** 207–209

Dietrich T, Onderka J, Bock F, Kruse FE, Vossmeyer D, Stragies R, Zahn G, Cursiefen C (2007) Inhibition of inflammatory lymphangiogenesis by integrin alpha5 blockade. *Am J Pathol* **171:** 361–372

Földi M, Strössenreuther R (2005) *Foundations of Manual Lymph Drainage*, 2004, 3rd edn, New York, USA: Elsevier

Friedl P, Wolf K, Lammerding J (2011) Nuclear mechanics during cell migration. *Curr Opin Cell Biol* **23:** 55–64

Friedland JC, Lee MH, Boettiger D (2009) Mechanically activated integrin switch controls alpha5beta1 function. *Science* **323:** 642–644

Fritz-Six KL, Dunworth WP, Li M, Caron KM (2008) Adrenomedullin signaling is necessary for murine lymphatic vascular development. *J Clin Invest* **118:** 40–50

Galvagni F, Pennacchini S, Salameh A, Rocchigiani M, Neri F, Orlandini M, Petraglia F, Gotta S, Sardone GL, Matteucci G, Terstappen GC, Oliviero S (2010) Endothelial cell adhesion to the extracellular matrix induces c-Src dependent VEGFR-3 phosphorylation without the activation of the receptor intrinsic kinase activity. *Circ Res* **106:** 1839–1848

Garmy-Susini B, Avraamides CJ, Schmid MC, Foubert P, Ellies LG, Barnes L, Feral C, Papayannopoulou T, Lowy A, Blair SL, Cheresh D, Ginsberg M, Varner JA (2010) Integrin alpha4beta1 signaling is required for lymphangiogenesis and tumor metastasis. *Cancer Res* **70:** 3042–3051

Garmy-Susini B, Varner JA (2008) Roles of integrins in tumor angiogenesis and lymphangiogenesis. *Lymphat Res Biol* **6:** 155–163

Geiger B, Spatz JP, Bershadsky AD (2009) Environmental sensing through focal adhesions. *Nat Rev Mol Cell Biol* **10:** 21–33

Goldman J, Conley KA, Raehl A, Bondy DM, Pytowski B, Swartz MA, Rutkowski JM, Jaroch DB, Ongstad EL (2007) Regulation of lymphatic capillary regeneration by interstitial flow in skin. *Am J Physiol Heart Circ Physiol* **292:** H2176–H2183

Hogan BM, Bos FL, Bussmann J, Witte M, Chi NC, Duckers HJ, Schulte-Merker S (2009) Ccbe1 is required for embryonic lymphangiogenesis and venous sprouting. *Nat Genet* **41:** 396–398

Hong YK, Lange-Asschenfeldt B, Velasco P, Hirakawa S, Kunstfeld R, Brown LF, Bohlen P, Senger DR, Detmar M (2004) VEGF-A promotes tissue repair-associated lymphatic vessel formation via VEGFR-2 and the alpha1beta1 and alpha2beta1 integrins. *FASEB J* **18:** 1111–1113

Ingber DE (2006) Cellular mechanotransduction: putting all the pieces together again. *FASEB J* **20:** 811–827

Jarvius M, Paulsson J, Weibrecht I, Leuchowius KJ, Andersson AC, Wählby C, Gullberg M, Botling J, Sjöblom T, Markova B, Ostman A, Landegren U, Söderberg O (2007) *In situ* detection of phosphorylated platelet-derived growth factor receptor beta using a generalized proximity ligation method. *Mol Cell Proteomics* **6:** 1500–1509

Karkkainen MJ, Haiko P, Sainio K, Partanen J, Taipale J, Petrova TV, Jeltsch M, Jackson DG, Talikka M, Rauvala H, Betsholtz C,

Alitalo K (2004) Vascular endothelial growth factor C is required for sprouting of the first lymphatic vessels from embryonic veins. *Nat Immunol* **5:** 74–80

Kajiya K, Hirakawa S, Ma B, Drinnenberg I, Detmar M (2005) Hepatocyte growth factor promotes lymphatic vessel formation and function. *EMBO J* **24:** 2885–2995

Klinghoffer RA, Sachsenmaier C, Cooper JA, Soriano P (1999) Src family kinases are required for integrin but not PDGFR signal transduction. *EMBO J* **18:** 2459–2471

Küchler AM, Gjini E, Peterson-Maduro J, Cancilla B, Wolburg H, Schulte-Merker S (2006) Development of the zebrafish lymphatic system requires VEGFC signaling. *Curr Biol* **16:** 1244–1248

Lei L, Liu D, Huang Y, Jovin I, Shai SY, Kyriakides T, Ross RS, Giordano FJ (2008) Endothelial expression of beta1 integrin is required for embryonic vascular patterning and postnatal vascular remodeling. *Mol Cell Biol* **28:** 794–802

le Noble F, Klein C, Tintu A, Pries A, Buschmann I (2008) Neural guidance molecules, tip cells, and mechanical forces in vascular development. *Cardiovasc Res* **78:** 232–241

Licht AH, Müller-Holtkamp F, Flamme I, Breier G (2006) Inhibition of hypoxia-inducible factor activity in endothelial cells disrupts embryonic cardiovascular development. *Blood* **107:** 584–590

Licht AH, Raab S, Hofmann U, Breier G (2004) Endothelium-specific Cre recombinase activity in flk-1-Cre transgenic mice. *Dev Dyn* **229:** 312–318

Machnik A, Neuhofer W, Jantsch J, Dahlmann A, Tammela T, Machura K, Park JK, Beck FX, Müller DN, Derer W, Goss J, Ziomber A, Dietsch P, Wagner H, van Rooijen N, Kurtz A, Hilgers KF, Alitalo K, Eckhardt KU, Luft FC *et al* (2009) Macrophages regulate salt-dependent volume and blood pressure by a vascular endothelial growth factor-C-dependent buffering mechanism. *Nat Med* **15:** 545–552

Mäkinen T, Norrmén C, Petrova TV (2007) Molecular mechanisms of lymphatic vascular development. *Cell Mol Life Sci* **64:** 1915–1929

Mammoto T, Ingber DE (2010) Mechanical control of tissue and organ development. *Development* **137:** 1407–1420

Nilsson I, Bahram F, Li X, Gualandi L, Koch S, Jarvius M, Söderberg O, Anisimov A, Kholová I, Pytowski B, Baldwin M, Ylä-Herttuala S, Alitalo K, Kreuger J, Claesson-Welsh L (2010) VEGF receptor 2/-3 heterodimers detected *in situ* by proximity ligation on angiogenic sprouts. *EMBO J* **29:** 1377–1388

Ny A, Koch M, Schneider M, Neven E, Tong RT, Maity S, Fischer C, Plaisance S, Lambrechts D, Héligon C, Terclavers S, Ciesiolka M, Kälin R, Man WY, Senn I, Wyns S, Lupu F, Brändli A, Vleminckx K, Collen D *et al* (2005) A genetic Xenopus laevis tadpole model to study lymphangiogenesis. *Nat Med* **11:** 998–1004

Okazaki T, Ni A, Ayeni OA, Baluk P, Yao LC, Vossmeyer D, Zischinsky G, Zahn G, Knolle J, Christner C, McDonald DM (2009) alpha5beta1 integrin blockade inhibits lymphangiogenesis in airway inflammation. *Am J Pathol* **174:** 2378–2387

Papusheva E, Heisenberg CP (2010) Spatial organization of adhesion: force-dependent regulation and function in tissue morphogenesis. *EMBO J* **29:** 2753–2768

Potocnik AJ, Brakebusch C, Fässler R (2000) Fetal and adult hematopoietic stem cells require beta1 integrin function for colonizing fetal liver, spleen, and bone marrow. *Immunity* **12:** 653–663

Rutkowski JM, Swartz MA (2007) A driving force for change: interstitial flow as morphoregulator. *Trends Cell Biol* **17:** 44–50

Saharinen P, Helotera H, Miettinen J, Norrmen C, D'Amico G, Jeltsch M, Langenberg T, Vandevelde W, Ny A, Dewerchin M, Carmeliet P, Alitalo K (2010) Claudin-like protein 24 interacts with the VEGFR-2 and VEGFR-3 pathways and regulates lymphatic vessel development. *Genes Dev* **24:** 875–880

Schulte-Merker S, Sabine A, Petrova TV (2011) Lymphatic vascular morphogenesis in development, physiology, and disease. *J Cell Biol* **193:** 607–618

Schwartz MA (2010) Integrins and extracellular matrix in mechanotransduction. *Cold Spring Harb Perspect Biol* **2:** a005066

Siekmann AF, Lawson ND (2007) Notch signalling limits angiogenic cell behaviour in developing zebrafish arteries. *Nature* **445:** 781–784

Söderberg O, Gullberg M, Jarvius M, Ridderstråle K, Leuchowius KJ, Jarvius J, Wester K, Hydbring P, Bahram F, Larsson LG, Landegren U (2006) Direct observation of individual endogenous protein complexes *in situ* by proximity ligation. *Nat Methods* **3:** 995–1000

Soriano P (1999) Generalized *lacZ* expression with the ROSA26 Cre reporter strain. *Nat Genet* **21:** 70–71

Srinivasan RS, Dillard ME, Lagutin OV, Lin FJ, Tsai S, Tsai MJ, Samokhvalov IM, Oliver G (2007) Lineage tracing demonstrates the venous origin of the mammalian lymphatic vasculature. *Genes Dev* **21:** 2422–2432

Strilić B, Kucera T, Eglinger J, Hughes MR, McNagny KM, Tsukita S, Dejana E, Ferrara N, Lammert E (2009) The molecular basis of vascular lumen formation in the developing mouse aorta. *Dev Cell* **17:** 505–515

Tammela T, Alitalo K (2010) Lymphangiogenesis: molecular mechanisms and future promise. *Cell* **140:** 460–476

Tammela T, Zarkada G, Wallgard E, Murtomäki A, Suchting S, Wirzenius M, Waltari M, Hellström M, Schomber T, Peltonen R, Freitas C, Duarte A, Isoniemi H, Laakkonen P, Christofori G, Ylä-Herttuala S, Shibuya M, Pytowski B, Eichmann A, Betsholtz C *et al* (2008) Blocking VEGFR-3 suppresses angiogenic sprouting and vascular network formation. *Nature* **454:** 656–660

Tanjore H, Zeisberg EM, Gerami-Naini B, Kalluri R (2008) Beta1 integrin expression on endothelial cells is required for angiogenesis but not for vasculogenesis. *Dev Dyn* **237:** 75–82

Tse JR, Engler AJ (2010) Preparation of hydrogel substrates with tunable mechanical properties. *Curr Protoc Cell Biol* **10:** 16 .1

Vlahakis NE, Young BA, Atakilit A, Sheppard D (2005) The lymphangiogenic vascular endothelial growth factors VEGF-C and -D are ligands for the integrin alpha9beta1. *J Biol Chem* **280:** 4544–4552

Wang Y, Botvinick EL, Zhao Y, Berns MW, Usami S, Tsien RY, Chien S (2005) Visualizing the mechanical activation of Src. *Nature* **434:** 1040–1045

Wang Y, Nakayama M, Pitulescu ME, Schmidt TS, Bochenek ML, Sakakibara A, Adams S, Davy A, Deutsch U, Lüthi U, Barberis A, Benjamin LE, Mäkinen T, Nobes CD, Adams RH (2010) Ephrin-B2 controls VEGF-induced angiogenesis and lymphangiogenesis. *Nature* **465:** 483–486

Wang Y, Oliver G (2010) Current views on the function of the lymphatic vasculature in health and disease. *Genes Dev* **24:** 2115–2126

Yaniv K, Isogai S, Castranova D, Dye L, Hitomi J, Weinstein BM (2006) Live imaging of lymphatic development in the zebrafish. *Nat Med* **12:** 711–716

Zhang X, Groopman JE, Wang JF (2005) Extracellular matrix regulates endothelial functions through interaction of VEGFR-3 and integrin alpha5beta1. *J Cell Physiol* **202:** 205–214

Zovein AC, Luque A, Turlo KA, Hofmann JJ, Yee KM, Becker MS, Fassler R, Mellman I, Lane TF, Iruela-Arispe ML (2010) Beta1 integrin establishes endothelial cell polarity and arteriolar lumen formation via a Par3-dependent mechanism. *Dev Cell* **18:** 39–51

